The United Graduate School of Veterinary Sciences, Yamaguchi University, Yamaguchi 753-8515, Japan.

TO WHOM IT MAY CONCERN

We hereby certify that, this is a typical copy of the original Doctor thesis of Mr. **Reda Farag Mohamed Rashed,** 2006.

Official seal

Professor Dr. ***Toshiharu Hayashi***
Dean of the United Graduate School of Veterinary Sciences, Yamaguchi University, Yamaguchi 753-8515, Japan.

MORPHOLOGICAL STUDY OF THE INFERIOR OLIVARY COMPLEX IN THE WATER BUFFALO, DONKEY, CAMEL AND CHICKEN

Reda Farag Mohamed Rashed

2006

The United Graduate School of Veterinary Sciences,
Yamaguchi University, Yamaguchi 753-8515,
Japan.

Contents

GENERAL INTRODUCTION

The morphology of the inferior olivary complex (IOC) has been demonstrated in many mammals (Kooy, 1916; Kappers et al., 1960; Taber, 1961; Moatamed, 1968; Breazile, 1967; Schild, 1970; Bowman and King, 1973; Bowman and Sladek, 1973; Martin et al., 1975; Watson and Herron, 1977; Rutherford and Gwyn, 1980; Saigal et al., 1983; Azizi and Woodward, 1987; Tan et al., 1995; Bozhilova - Pasirova and Ovtscharoff,. 2000; Bukowska et al., 2002). There are relatively few studies on this nuclear complex in large animals including the water buffalo, donkey and camel.

In most of studied mammals, the IOC is divided into three main nuclei; medial and dorsal accessory olivary nuclei (MAO and DAO, respectively), and a principal olivary nucleus (PO) and four small cell groups; the dorsal cap (DC), the ventro - lateral outgrowth (VLO), the nucleus β and the dorso - medial cell column (DMCC). However, the marsupial's IOC consists of the same nuclei but their relative positions are different from other mammals (Martin et al., 1975; Watson and Herron, 1977).

Recently, the IOC has been compartmentalized by the olivocerebellar projections using tracer techniques (Tan et al., 1995). It is generally recognized that the IOC is the sole source of the climbing fibers (Brodal et al., 1950; Szentagothai and Rajkovits, 1959; Desclin, 1974; Freedman et al., 1977), and nearly all of the neurons in the IOC are probably projection neurons to the cerebellum (De Zeeuw et al., 1998). A single

olivocerebellar fiber projects with multiple climbing fibers to a single narrow longitudinal band - shaped area in the cerebellar cortex and, with its axon collaterals, to a small area in the cerebellar nuclei (Sugihara et al., 1999). Each climbing fiber innervates a single Purkinje cell (Eccles et al., 1966). Each olivocerebellar fiber branches into about 4 - 7 (rat) to 14 - 17 (human) climbing fibers (Rashed et al., 2005). Thus we can estimate the number of Purkinje cells by direct counting or by the neuronal numbers of the IOC. Furthermore we can reckon a more detailed role of each main nucleus by morphometrical observations of the neuronal number in each main nucleus of the IOC. We discussed that neuroanatomical results of the IOC in small mammals could be applicable to the large mammals like the water buffalo, camel and donkey.

The avian IOC consists of a large dorsal and a small ventral lamellae. It has been believed on the basis of the morphological appearance that the ventral lamella corresponds to the PO, the lateral and medial parts of the dorsal lamella are the homologue of the DAO and MAO of mammals, respectively (Kuhlenbeck, 1975). In the chapters I, the morphology of the IOC in the water buffalo was studied and compared with those of other mammals. In addition, the neuronal count and neuronal density of each nucleus of the IOC was estimated. In the chapters II and III, the morphology of the IOCs in the donkey and camel were morphologically investigated in comparison with those of other mammals.

In the chapter IV, the numerical ratio of the IOC neurons to Purkinje cells (PCs) in the chicken was elucidated.

Chapter I

Qualitative and quantitative studies of the inferior olivary complex in the water buffalo (*Buballus bubalis)*

SUMMARY

The shape and neuronal number of the inferior olivary complex (IOC) were determined in the water buffalo (*Buballus bubalis*). The configuration and interrelations of the IOC compartments were ascertained by investigating serial sections through the whole rostro-caudal extent of the IOC. Nissl-stained celloidin sections of six water buffalo's brainstems were used. The IOC in the water buffalo consisted of three major nuclei and four small cell groups. The medial accessory olivary nucleus (MAO) had the longest rostro-caudal extent as well as the highest number of neurons (98,000±3,000). Although the total area of the principal olivary nucleus (PO) was smaller than the area of the dorsal accessory olivary nucleus (DAO), the PO had the second largest neuron number. The total number of neurons on both sides of the IOC was 211,000 ±7,000 cells. The average neuron density was 3,000 cells / mm^3. Although the size of the PO relatively increases while the size of MAO decreases with the development of the cerebellar hemispheres, the IOC in most mammals maintains a similar structure except for the higher primate and marsupial. The water buffalo IOC showed close similarities to those of the majority of mammals including rats as follow; the main part of the MAO consists of three subgroups (a, b and c), the DAO is Boomerang-shaped while the PO is U-shaped structure.

INTRODUCTION

Recently, the IOC has been compartmentalized by the olivocerebellar projections using tracer techniques (Tan et al., 1995). Consequently we can correlate roughly the morphological structures that are shown by Nissl-stained sections, with the compartments by neural circuits of the IOC. However, these tract tracing methods are limited in small mammals including rats, rabbits and cats. More over, there have been relatively few studies on this nuclear complex in large animals including the water buffalo (as a prevalent ruminant in Asia and Africa).

In this study we described the morphology of the IOC in the water buffalo, to which it is very difficult to apply tract tracing methods for size, and compared the IOC of the water buffalo with other mammals. We discussed that neuroanatomical results of the IOC in small mammals could be applicable to the large mammals like the water buffalo.

Each climbing fiber innervates a single Purkinje cell. Each olivocerebellar fiber branches into about 4 - 7 (rat) to 14 - 17 (human) climbing fibers (Rashed et al., 2005). Thus we can estimate the number of Purkinje cells by the neuronal numbers of the IOC. Further more we can reckon a more detailed role of each main nucleus by getting to know the neuronal number in each main nucleus of the IOC. To this end, neuronal cell counts were performed in the IOC of the water buffalo.

MATERIALS AND METHODS

Six water-buffalo (*Buballus bubalis)* calves, 3 to 4 months old, were obtained from a slaughter house in Egypt. The brainstems including the IOC were removed, fixed in 10% formalin for three weeks, dehydrated and embedded in 10% celloidin. The specimens were serially sectioned at 50 μm thick in the transverse plane and stained with toluidine blue or cresyl echt violet.

Histology and procedure for neuron counts: The nuclear configuration was mapped using a drawing tube. The sections were observed under a light microscope at a final magnification of 100× for cell counting. The IOC neurons were counted in every tenth section on both the right and left sides of each animal. All neurons present in a given section were counted, whether or not a nucleolus could be identified. The total neuron number of the IOC was then calculated by the method of Escobar et al. (1968) as follows: the number of neurons (A) in each section counted was multiplied by half the number of sections not counted (B) between the section counted and the next counted section (Escobar et al., 1968; Ruigrok and Voogd, 2000). By adding the products of AxB/2 for all sections counted, the estimated total number of neurons in the IOC of each specimen was obtained. The three-dimensional shapes of IOC compartments were obtained from the cross sections in Fig.1 by overlapping the sections in an image processor, proceeding form rostral to caudal direction (Fig. 3).

Procedure for neuron density: The neuron density was obtained by projecting the microscopic sections onto a video micrometer [VM-29; Olympus, Tokyo, Japan] at a final magnification 90×. The relative areas of each nucleus and small cell group of the IOC were measured in every tenth section on the left sides of four cases (Table 1). The number of neurons per square millimeter in each counted section was obtained, and then the number of neurons per cubic millimeter was obtained by multiplying the mean number of neurons / mm^2 by the Escobar coefficient (Escobar, et al., 1968) from the following formula:

Escobar coefficient = 1,000 mm/ (section thickness x 2*)

2*: the neuron count for one section is equal to the neuron count for two successive sections (Escobar, et al., 1968).

In this study, the Escobar coefficient = 1,000 / (50x2) = 10

RESULTS

Morphology of IOC: Three major nuclei, the MAO, DAO and PO, in addition to four small cell groups, were clearly detected in the water buffalo IOC (Figs. 1, 2). The IOC extended for a rostro-caudal extension of 10 ± 0.5 mm.

The MAO was the first nucleus to appear in the caudal pole of the IOC. Among the three major nuclei, the MAO had the longest rostro-caudal dimension extending over approximately 7.5 mm. At the caudal aspect of the MAO, three separate groups could be distinguished, a, b and c, from laterally to medially. Group b appeared as an independent cell cluster at the most caudal level (Fig. 1 - 1). More rostrally group c fused with the nucleus β (Fig. 1 - 5) and then a-c groups with the nucleus β formed one horizontal sheet (Fig. 1 - 6). More rostrally, group c separated from the MAO (Fig. 1 - 8), diminished in size, and then disappeared (Fig. 1 - 10). At the rostral half of IOC, the MAO (a combination of groups a and b) decreased in size and finally disappeared (Fig. 1 - 15). The cytoarchitectural boundaries of groups a, b and c were rather clear in the caudal half of the MAO but obscure in the rostral half.

The DAO appeared medially as thin sheet of cells dorsally to the MAO and lateral to the VLO (Fig. 1 - 6). This sheet of neurons extended laterally (Fig. 1 - 7) and then bent ventrally (Fig. 1 - 8). The new growing ventral lamina of the DAO increased in size and extended medially, simultaneously with the diminishing of the dorsal lamina until the DAO took a medial

position (Fig. 1 - 9, 1 - 12). More rostrally, the medial part of the DAO had a connection with the dorsal lamella of PO (Fig. 1 - 15). Caudal to the rostral pole of the IOC, the DAO lost its connection with the dorsal lamella of PO (Fig. 1 - 18) and continued to form the rostral pole of the IOC.

The PO extended through the rostral half of the IOC with its dorsal lamella (DL), appearing as a ventrolaterally oriented band (Fig. 1 - 11). More rostrally, the PO consisted of dorsal and ventral lamellae (VL), forming a U-shape with a medial hilus (Fig. 1 - 13). The DL, somewhat larger than the VL, decreased in size, and eventually disappeared (Fig. 1 - 18). The VL shared the DAO forming the rostral pole of the IOC.

The DC appeared as a distinct cell group at caudal levels of the IOC (Fig. 1 - 3). The DC was situated dorsal to group c and then moved dorsally (Fig. 1 - 4). The DC moved laterally, persisted for a few sections and then decreased in size and disappeared (Fig. 1 - 7). The nucleus β appeared as the dorsal extension of group c ventral to the DC. The VLO appeared as a separate small cell cluster in between the DC and the nucleus β (Fig. 1 - 4). More rostrally, the VLO pushed the DC laterally, and then continued rostrally between the nucleus β and the DAO (Fig. 1 - 7). The DMCC appeared as a separate cell cluster situated medially in relation to the ventral lamella of the PO and dorsomedially to MAO (Fig. 1 - 14). The DMCC continued rostrally for a short distance until it disappeared (Fig. 1 - 16).

Neuron number and density in IOC: The neuron numbers in the IOC of the water buffalo was estimated (Table 1). The neuron numbers were statistically same in the right (105,500 ± 3,900 cells) and left (105,600 ± 3,500 cells) sides of the IOC. The neuron density in the IOC of the water buffalo was calculated to be 3,000 cells / mm^3 in mean (Table 1)

Among the three major nuclei, the MAO had the largest cell number (Table 1). Although the relative area of the PO was smaller than that of the DAO, the PO had the second largest neuron number (Table 1). The three-dimensional shapes of each nucleus of the IOC were illustrated in Fig. 3.

Table 1

Cell counts, relative area and the neuronal density of each nucleus in the both side of the IOC of the water buffalo.

Major Nuclei		MAO		DAO		PO		Total
Sub-Nuclei	a, b and c	Nucleus β	DMCC	DAO	PO	DC	VLO	
Subtotal	83,000	12,000	3,000	54,000	47,000	4,000	7,000	
Total number Means ± SD*		98,000 ±3,000		54,000 ± 6,000		58,000 ± 2,000		211,000 ± 7,000
CV**		3%		10%		3%		3%
Relative neuron number		47%		26%		27%		
Relative area		35%		43%		23%		
Neuronal density (cells / mm3)		3,700 ± 800		1,900 ± 300		3,200 ± 200		3,000 ± 400

SD*: Standard Deviation **CV****: Coefficient of Variation.

Figures and figure legends

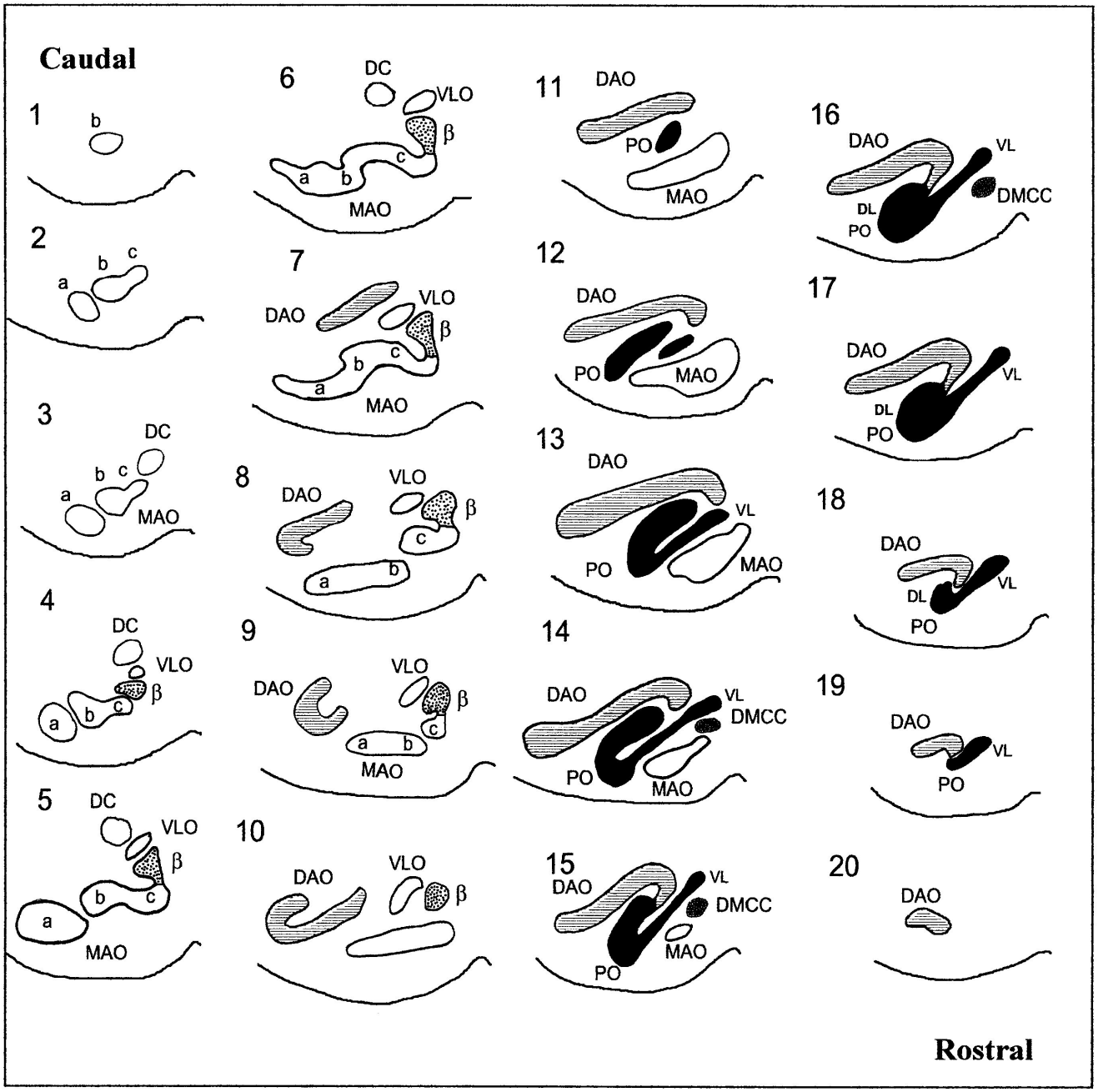

Fig.1

Line drawings of cross-section of the left medulla oblongata illustrating positions and relations among the subnuclei of IOC in the water buffalo. Abbreviations: DAO; dorsal accessory olive, MAO; medial accessory olive, PO; principal olive, a-c; groups a-c of MAO, β; nucleus β, DC; dorsal cap, VLO; ventrolateral outgrowth, DMCC; dorsomedial cell column, DL; dorsal lamella of PO, VL; ventral lamella of PO.

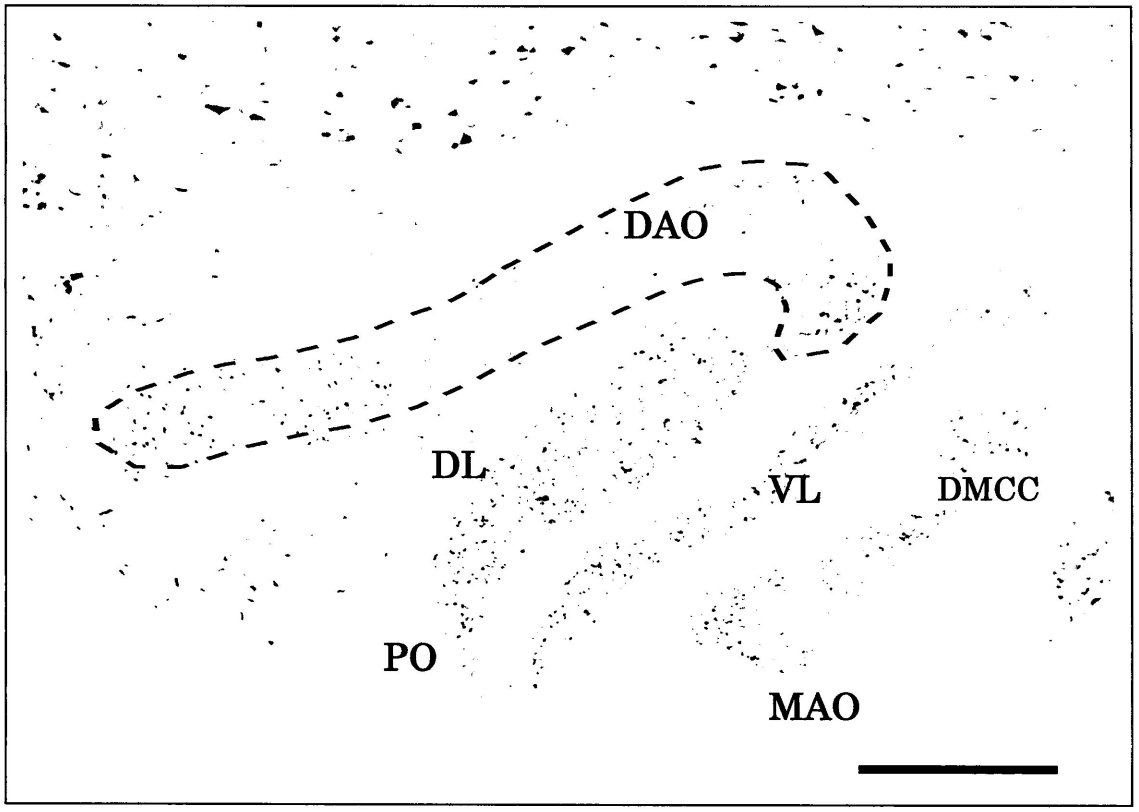

Fig. 2 A photomicrograph of the three major nuclei of the IOC. The photo corresponds to the level 14 in Fig. 1. Abbreviations are the same as Fig. 1. The scale bar = 1 mm.

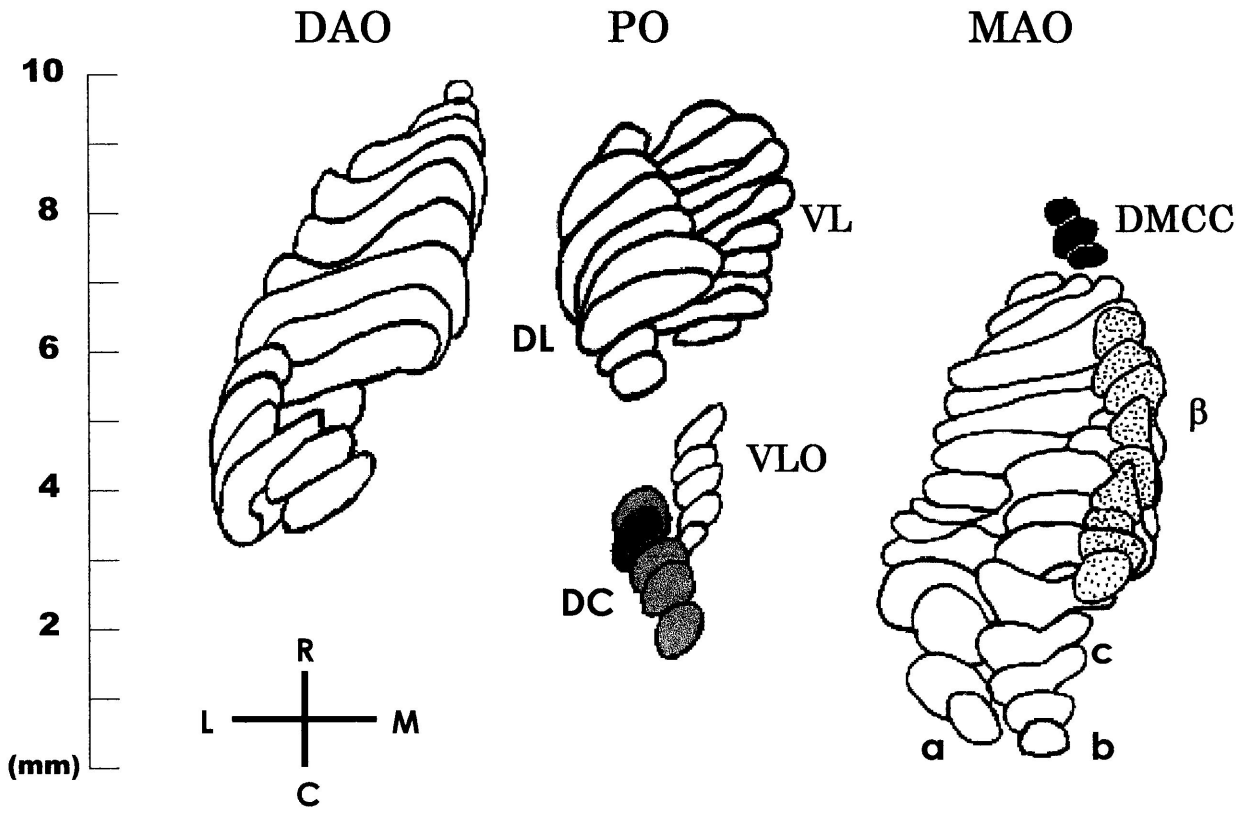

Fig. 3 Three—dimensional shapes of the IOC compartments in the water buffalo. M: medial; L: lateral; R: rostral; C: caudal. Other abbreviations are the same as Fig. 1.

DISCUSSION

The main part of the MAO is divided into rostral and caudal halves, based on the olivocerebellar projections (Groenewegen, and Voogd, 1977; Groenewegen et al., 1979; Ruigrok, and Voogd, 2000). The caudal half consists of three groups, a, b and c with clear outlines, while the rostral half consists of two groups, a and b, groups which are merged into one sheet in many mammals (Azizi and Woodward, 1987; Watson. and Herron, 1977). Another two isolated groups are added to the MAO; the nucleus β and its rostral continuation. The DMCC appears as a separate cell cluster dorsal to the MAO (Azizi, and Woodward, 1987; Bowman and Sladek, 1973; Breazile, 1967; Bukowska et al., 2002; Taber, 1961; Tan et al., 1995). The MAO in the water buffalo showed close similarities in shape and construction to those of other mammals including the rat, pig, goat, cat and horse. The DAO in mammals, consists of one lamella, except for the rat, in which it consists of two lamellae joined laterally (Azizi and Woodward, 1987; Schild, 1970; Delhaye-Bouchaud et al., 1985). The caudal tail of the DAO in the rat (Azizi and Woodward, 1987; Schild, 1970), cat (Brodal, 1940), goat and horse (Kooy, 1916.) and pig (Breazile, 1967) start medially, then shifts laterally and then more rostrally extends medially again. The DAO consists of a "boomerang-shaped" caudal tail and a rostral body. The DAO in many mammals except sheep is partially continuous with the dorsal lamella and the ventral lamella of the PO (Breazile, 1967; Brodal et al., 1975;

Groenewegen et al., 1979; Mlonyeni, 1973). The DAO in the water buffalo IOC was "boomerang-shaped" in transverse sections and was composed of a single lamella with the dorsal lamella of the PO. Generally, the PO consists of the dorsal and ventral lamellae, which are joined at their lateral bend (Azizi and Woodward, 1987; Breazile, 1967; Bukowska et al., 2002; Groenewegen et al., 1979; Gwyn et al., 1977; Martin et al., 1975; Mlonyeni. 1973; Saigal et al., 1983). In the higher primates, the PO is well developed with many folds (Bowman. and Sladek, 1973; Kappers et al., 1960). The VLO and the DC are considered as a caudal continuation of the PO (Brodal and Kawamura, 1980; Ruigrok and Voogd, 2000). The DC in many mammals appears as a dorsal extension from group c, and then elongates ventrolaterally at rostral levels to form the VLO (Azizi and Woodward, 1987, Bowman. and Sladek, 1973; Brodal et al., 1975; Bukowska et al., 2002; Flumerfelt and Hrycyshyn, 1986). The PO in the water buffalo that consisted of two lamellae had no flexure and occupied only the rostral half of the IOC. The dorsal lamella was larger than the ventral lamella similar to that of the elephant PO (Armstrong, 1974). Although the DC and the VLO in the water buffalo had an orientation similar to that of many mammals, the VLO was not an elongation of the DC.

In the present study, since the IOC in the water buffalo showed close morphological similarities to those of the majority of mammals including rats, we conclude that the olivocerebellar and olivonuclear

projections of the water buffalo IOC probably are similar to those of other mammals. The total numbers of IOC neurons have been estimated at about 909,000, 1,025,000 or 1,060,000 in humans (Escobar et al., 1968; Farhad, 1966., Futami and Okamoto, 1968), 27,000 in the vampire bat (Escobar et al., 1968), 140,000 or 150,000 in the cat (Escobar et al., 1968; Mlonyeni, 1973] and 49,000 or 57,000 in the rat (Delhaye—Bouchaud et al., 1985; Schild, 1970), respectively. The IOC in the water buffalo contained 211,000 neurons in total. Thus the IOC neurons in the water buffalo appeared to be more numerous than in the cat and fewer than in humans.

Generally, the MAO is the largest nucleus of the IOC in most mammals studied except for higher primates, in which the PO is the largest nucleus (Armstrong, 1974; Azizi, and Woodward, 1987, Farhad, 1966). Numerical studies show that the MAO, DAO and PO contain neurons at proportions of 10%, 3% and 86%, respectively, in humans (Farhad, 1966), 49%, 24% and 27% or 46%, 25% 29% in the rat (Delhaye—Bouchaud et al., 1985 Schild, 1970) and 47%, 26% and 27% in this study, thus, in addition to the morphological similarity to the rat IOC, the water buffalo was also similar to the rat in the proportion of its three major nuclei.

Estimates have been made of the packing density of cells within the IOC. It is estimated as 65,000 cells /mm^3 in the vampire bat and carp (Bozhilova - Pasirova and Ovtscharoff, 2000; Escobar et al.,

1968), 44,000 cells /mm^3 in the rat (Escobar et al., 1968, Schild, 1970), 28,000 cells /mm^3 in the pigeon (Bozhilova-Pasirova and Ovtscharoff, 2000), 23,000 cells /mm^3 in the ground squirrel [Bozhilova-pasirova and Ovtscharoff, 2000), 8,000 ~ 15,000 cells /mm^3 in the cat (Bozhilova-pasirova and Ovtscharoff, 2000; Escobar et al., 1968) and 5,000 ~ 15,000 in human (Bozhilova-Pasirova and Ovtscharoff, 2000)., Escobar et al., 1968). A glance at these neuron density shows that the densities correlate inversely with body weight. The neuron density in the IOC of the water buffalo was 3,000 cells /mm^3. Since the water buffalo is markedly heavier than the human, the neuron density of the water buffalo IOC may be lower than that of humans.

CHAPETR II

Morphological study on the inferior olivary complex of the donkey (*Equus asinus*)

SUMMARY

This study provided basic data on the normal structure of the inferior olivary complex (IOC) of the donkey (*Equus asinus*) at the light microscopic level. In common with that of other mammals, the donkey IOC consisted of three major nuclei and four minor groups of cells. The former was comprised of the medial and dorsal accessory olive (MAO and DAO, respectively) and the principal olive (PO), and the MAO was comprised of the dorsal cap, nucleus β, ventrolateral outgrowth and dorsomedial cell column. The MAO had the longest rostral to caudal representation and formed the caudal pole of IOC. The DAO was located dorsally to the MAO and occupied about the rostral four fifths of the IOC and its caudal part was low in neuronal density with obscure outline. In the rostral half, the DAO bended ventrally and merged with the dorsal lamella of PO. More rostrally, the DAO lost its connection with the dorsal lamella and then conversely connected with the ventral lamella of PO. The DAO formed the rostral pole of the IOC. The dorsal cap was a small group of cells. Overall, the donkey IOC is similar to those of the other mammals.

INTRODUCTION

It is well known that the IOC is the sole source of the climbing fibers that innervate the Purkinje cells of the cerebellar cortex (Szentagothai and Rajkovits, 1959; Desclin, 1974; Whitworth and Haines, 1986). A single neuron in the IOC projects with multiple climbing fibers to a single narrow longitudinal band-shaped area in the cerebellar cortex and, with its axon collaterals, to a small area in the cerebellar nuclei (Sugihara et al., 1999), thus defining functional compartmentalization of the cerebellar system in the vermis and hemispheres (Sugihara et al., 2001) that is much finer than the A − D zonation of the olivocerebellar projection revealed by mass labeling (Groenewegen and Voogd, 1977; Voogd, 2003).

The precise morphology of IOC has not been investigated in large animals such as donkey. More over, in any morphological and functional study of the IOC, it is essential to elucidate the olivocerebellar and olivonuclear projections originating from each IOC region. However, it is very difficult to apply a tract tracing methods to large mammals such as the donkey. The aim of this study is to describe the cytoarchitecture of the donkey IOC and to discuss its features in comparison with those in the IOC of the other mammals.

MATERIALS AND METHODS

A total of five donkeys (*Equus asinus),* 4-6 months old, were used in this study. The animals were anesthetized with an overdose of pentobarbital sodium, and then perfused with physiological saline followed by 10% formalin via the carotid artery. The brain stems were removed, post-fixed in the same fixative for three days or more, dehydrated using ascending series of ethanol, and embedded in celloidin. The brain stem was serially cut in the transverse plane at 50 μm thick. Serial sections were stained with toluidine blue or cresyl violet.

RESULTS

The terminology for anatomical structures used in this paper would imply homology in other mammals. The IOC dimensions were about 11.0 mm rostro-caudally, about 5.5 mm dorso-ventrally, and about 3.8 mm medio-laterally, in average. Three major nuclei, MAO, DAO and PO, as well as four small cell groups were clearly detected in the donkey IOC (Figs. 1, 2).

Of the three major nuclei, the MAO had the longest rostral to caudal representation, extending over approximately the caudal four fifths of the total IOC length. At the caudal aspect of the MAO, three separate groups may be distinguished, groups a, b and c, from laterally to medially (Fig. 2-A and B). Group b appeared as an independent cell cluster at the most-caudal level, forming the caudal pole of the IOC (Fig. 1-1). Slightly more rostrally, the other two groups developed from group b, group a laterally and group c medially. These three groups increased gradually in size and more rostrally formed totally a horizontal sheet of cells (Fig.1- 5, 6). More rostrally, the horizontal sheet assumed an S-shaped curve (Fig. 1-10, 11). At the level of the caudal third of the IOC, a constriction appeared between group b and group c which subsequently separated these groups from each other (Fig.1-13). More rostrally, group c shifted medially, diminished in size, and then disappeared (Fig.1-17). At approximately the rostral two-third of the IOC, groups a and b fused and then the MAO gradually decreased in size and finally disappeared (Fig.1-32). The cytoarchitectural boundaries of groups a, b and c were rather clear in the caudal half of the MAO but obscure in the rostral half.

The DAO appeared medially (Figs. 1-6 to 10, Fig. 2A) as a small cell cluster with a low nerve cell density. More rostrally, the DAO moved laterally with increased nerve cell density (Fig.1-12). The DAO bended ventrally and this bended ventral portion increased in size and migrated medially (Fig.1-16), simultaneously with diminishing of the dorsal portion of DAO (Fig.1-18). The medial end of the DAO had a connection with the dorsal lamella of PO (Fig.1-19) and this connection was interrupted over a certain distance of the IOC (Fig.1-26 to 1-27). More rostrally, the DAO had lost its connection with the dorsal lamellae of PO, and then DAO formed a connection with the ventral lamella of PO slightly caudal to the rostral end of the IOC (Fig.1-35).

The PO extended through the rostral half of the IOC with its dorsal lamella appeared as a ventrolaterally oriented band (Fig.1-18). More rostrally, the PO consisted of the dorsal and ventral lamellae, forming a U-shape with the medial hilus (Fig.1-22). The two lamellae were nearly equal in size. The ventral lamina partially divided into two parts, a ventro-lateral part continued with the dorsal lamella and a dorso-medial part (Fig. 1-25 to 28). These parts merged again into one lamella. At the rostral levels, the combined PO and DAO assumed an inverted S-shaped form (Fig.1-22 to 33, 2D). More rostrally, the dorsal lamella became detached from the DAO and then the ventral lamella joined to the DAO (Fig.1-35). The dorsal lamella decreased in size, and then disappeared (Fig.1-37) and then, the ventral lamella disappeared leaving the DAO formed the rostral pole of IOC (Fig. 1-38).

Four small cell groups were composed of the DC, nucleus β, VLO and DMCC. The DC initially appeared just dorsal to group c as a discrete cluster of cells, but soon lay just dorsal to the nucleus β (Fig. 1-5). This was very small, extending over a few sections (Fig. 1-5 to 7). The VLO appeared laterally to the DC and dorsally to nucleus β as a small and distinct cell cluster (Fig. 1-7). More rostrally, the VLO was located between the nucleus β and the DAO (Figs. 1-11 to 16). The DC and VLO was a distinct subdivision from first to last. The nucleus β initially was fused ventrally with group c and located just ventral to the DC (Fig. 1-7). Further rostrally the nucleus β separated from group c and disappeared at approximately the middle of the IOC (Fig. 1-20). Just after the disappearance of the DC, the nucleus β was situated ventral to the VLO. Further rostrally, the nucleus β shifted to the medial side of the VLO and then was located medially to the DAO after the disappearance of the VLO (Fig. 1-17 to 19). The DMCC appeared in the rostral half of the IOC in the position of nucleus β (Fig.1-23). The DMCC was appeared as a separate cell cluster situated medially to the ventral lamella of the PO and dorsally to the MAO.

The three-dimensional shapes of each subnucleus of the donkey IOC and an unfolded representation of the subnuclei of the IOC were illustrated in Fig. 3A and 3B, respectively.

Figures and figure legends

Fig. 1.

Line drawings of cross section of the medulla oblongata illustrating positions and relations among subnuclei of IOC in the donkey. DAO; dorsal accessory olive, MAO; medial accessory olive, PO; principal olive, a-c; groups a-c of the MAO, β; nucleus β, DC; dorsal cap, VLO; ventrolateral outgrowth, DMCC; dorsomedial cell column, DL; dorsal lamella of PO, VL; ventral lamella of PO.

Fig. 2. Light micrographs of transverse section of the IOC.

(A) Light micrograph illustrating S-shaped MAO.

(B) Light micrograph illustrating the division of the MAO.

(C) Light micrograph illustrating the three major nuclei of the IOC.

(D) Light micrograph illustrating inverted S-shape made by DAO and PO.

Fig. 2-A corresponds to Fig. 1-10.

Fig. 2-B corresponds to Fig. 1- 14

Fig. 2-C corresponds to Fig. 1- 26

Fig. 2-D corresponds to Fig. 1-30

Fig. 3

A: Three-dimensional shapes of MAO, PO, and DAO in the donkey IOC.

B: Unfolded representation of the IOC subnuclei. In the DAO dashed areas are low in neuronal density and obscure in its contour. See figure 1 for abbreviations

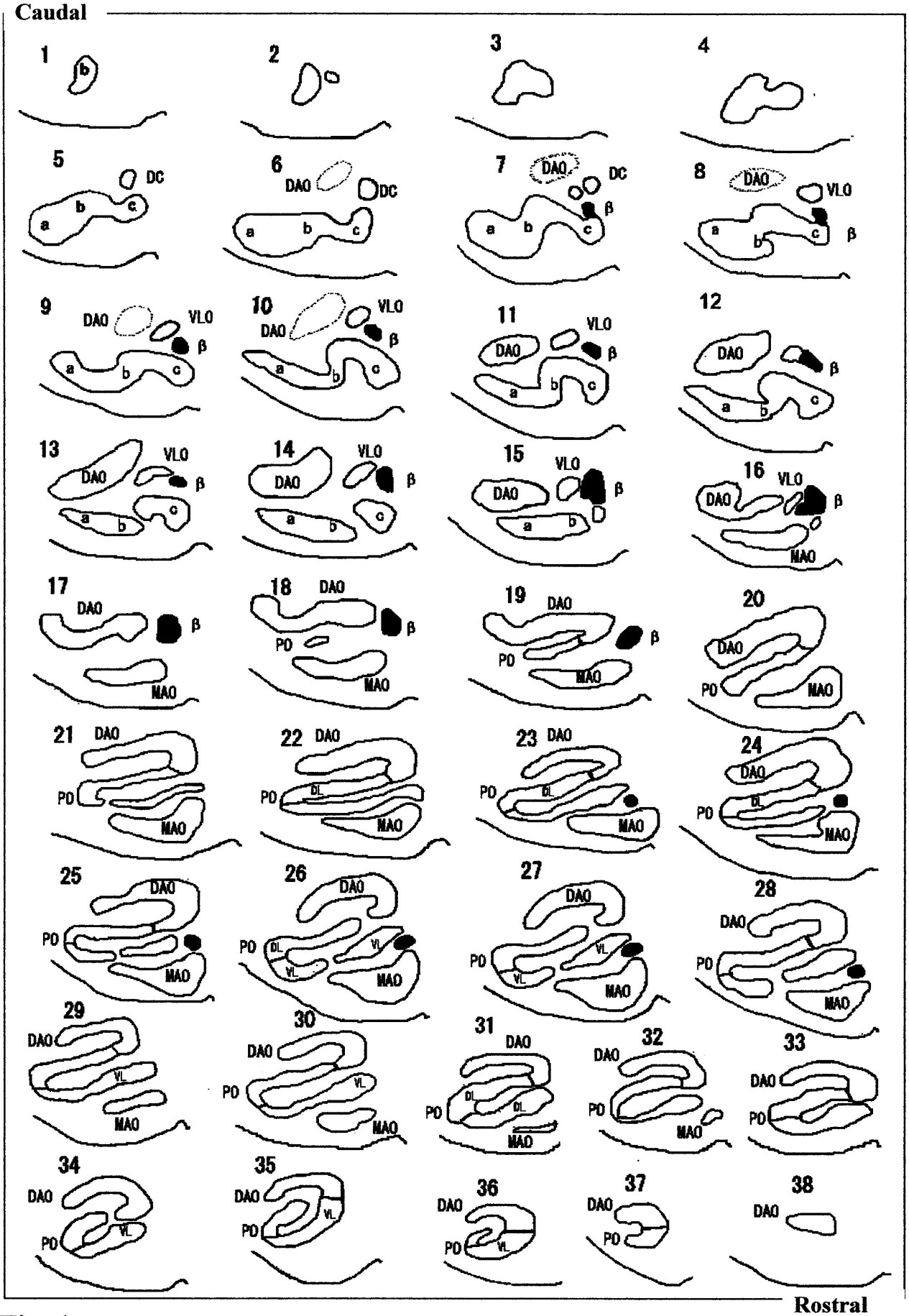
Caudal
1
2
3
4
5
DC
6
DAO
DC
7
DAO
DC
8
DAO
VLO
9
DAO
VLO
10
DAO
VLO
11
VLO
12
13
VLO
14
VLO
15
VLO
16
VLO
MAO
17
DAO
18
DAO
19
DAO
20
DAO
PO
MAO
21
DAO
PO
MAO
22
DAO
PO
DL
MAO
23
DAO
PO
DL
MAO
24
DAO
PO
DL
MAO
25
DAO
PO
MAO
26
DAO
PO
DL
VL
MAO
27
DAO
PO
VL
MAO
28
DAO
PO
MAO
29
DAO
VL
MAO
30
DAO
PO
VL
MAO
31
DAO
PO
DL
DL
MAO
32
DAO
PO
MAO
33
DAO
PO
34
DAO
PO
VL
35
DAO
PO
VL
36
DAO
PO
VL
37
DAO
PO
38
DAO
Rostral

Fig. 1

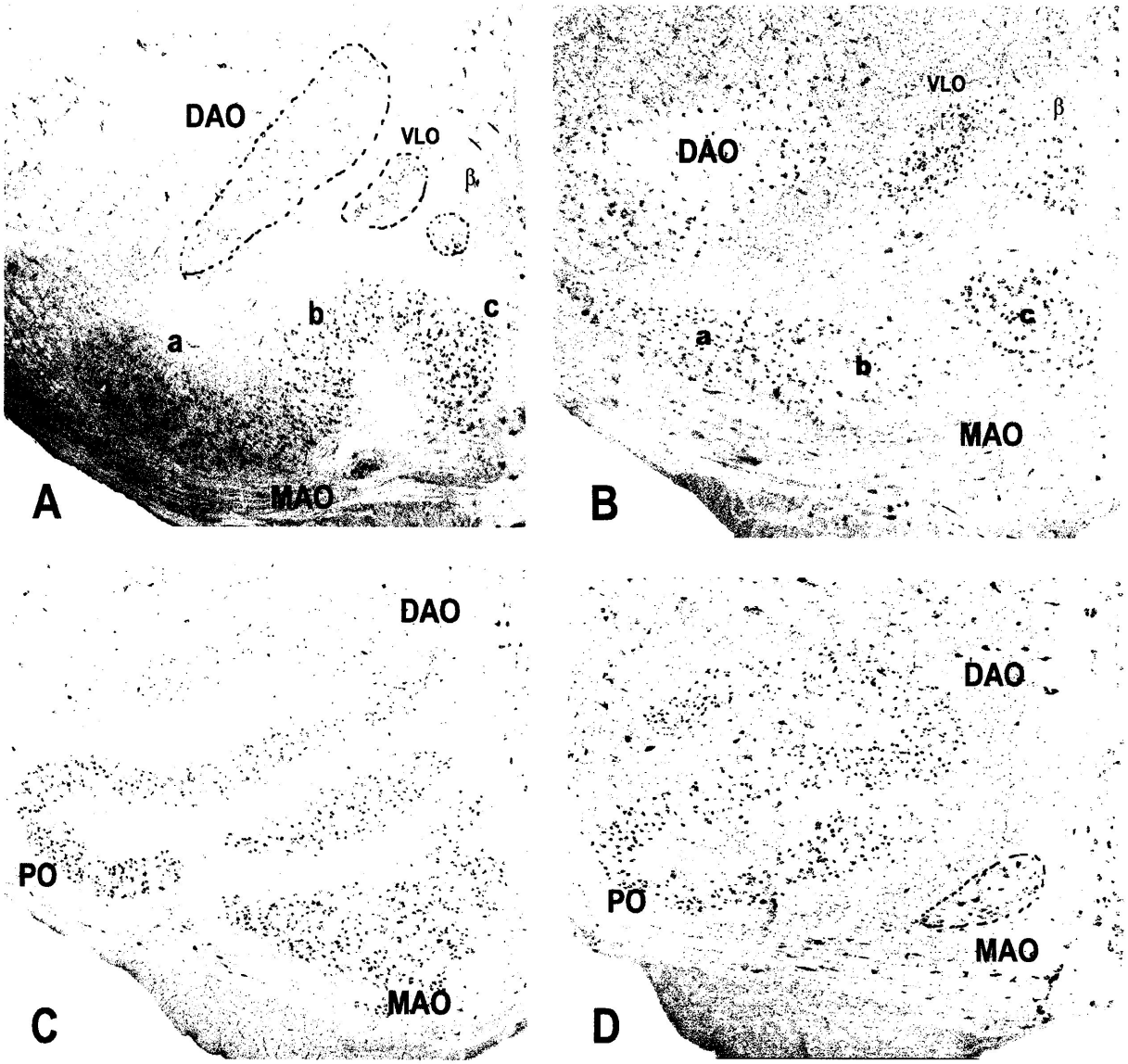

Fig. 2

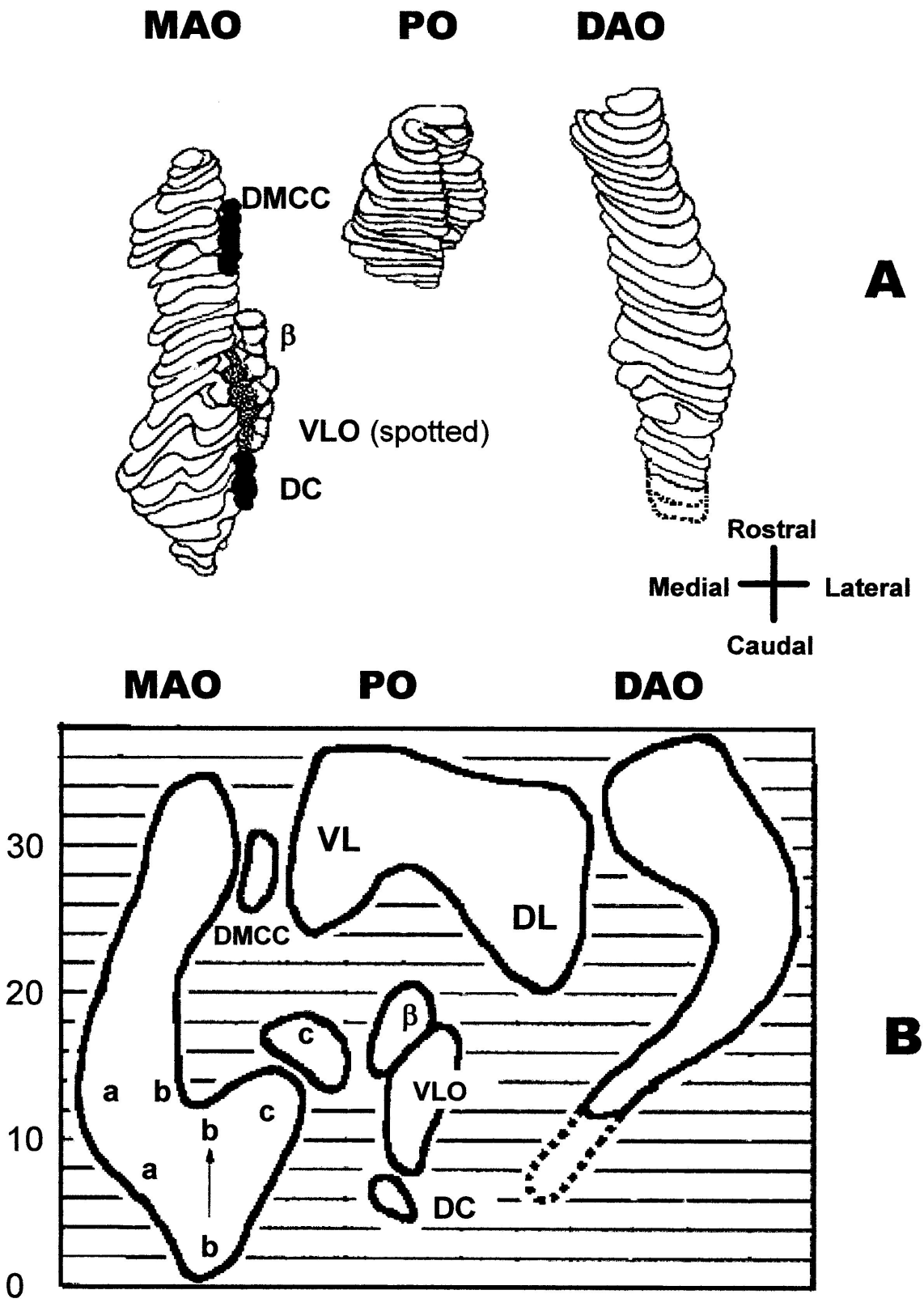
MAO
PO
DAO
DMCC
β
VLO (spotted)
DC
A
Rostral
Medial
Lateral
Caudal
MAO
PO
DAO
30
20
10
0
VL
DL
DMCC
β
c
a
b
c
VLO
b
a
b
DC
B

Fig. 3

DISCCUSSION

In most mammals except for the higher primates, the MAO is the largest of the three main nuclei of the IOC (Kooy, 1916; Moatamed, 1968; Armstrong, 1974; Azizi and Woodward, 1987). The MAO is generally subdivided into rostral and caudal parts, or rostral, intermediate and caudal parts based on the olivocerebellar and olivo-cerebellar nuclear projections (Groenewegen and Voogd, 1977; Groenewegen et.al, 1979; Flumerfelt and Hrycyshyn, 1986; Azizi and Woodward, 1987; Voogd and Glickstein, 1968; Ruigrok and Voogd, 2000; Voogd, 2003; Voogd and Ruigrok, 2004). The caudal MAO is further subdivided into three separate groups a, b, and c from laterally to medially. In this study, the donkey MAO was the longest of the three main nuclei in the IOC in rostrocaudal length. The caudal part of donkey MAO consisted of groups a, b and c, with group b forming the caudal pole of the IOC. It is a fact that the subdivisions of MAO cannot be readily recognized in Nissl-stained sections, but the donkey MAO is similar to that of the rat or other mammals.

The DAO is generally a small nucleus of the IOC and consists of one lamella. The rat DAO exceptionally consists of two lamellae joined laterally (Schild, 1970; Delhaye-Bouchaud et al., 1985; Azizi and Woodward, 1987)). In the most mammals, the DAO is continuous with the dorsal lamella of the PO, and more rostrally becomes continuous with the ventral lamella of the PO (Kooy, 1916; Brodal et al., 1975). In the pig, this configuration is reversed (Breazile, 1967), and the sheep DAO has no connection with the PO (Saigal et al., 1983). The DAO in

many mammals including the rat, pig, goat, cat and horse starts medially in the caudal end, then shifts laterally and then more rostrally extends medially again (Kooy, 1916). The donkey DAO was basically similar to many other mammals in location and relation with the PO. The donkey DAO was composed of a single lamella to blend with the dorsal lamella of the PO and in a part rostrally with the ventral lamella. However, its caudal tail was unclear in contour because of low neuron density.

The PO has much the same shape in all mammals. It is situated at the rostral part of the IOC and never extends as far caudalward as accessory olives. The PO consists of a dorsal and ventral lamella, which are joined at their lateral bend. The PO is the smallest nucleus in the rodent IOC and the largest in the human IOC (Moatamed, 1968; Armstrong, 1974; Azizi and Woodward, 1987). In primates, the PO is well developed and folded (Kappers et al., 1960; Bowman and Sladek, 1973). Numerical studies show that the MAO, DAO and PO contain neurons at proportions of 10%, 4% and 86%, respectively, of the total number of neurons of the human IOC (Moatamed, 1968), and 49%, 24% and 27% (Schild, 1970) or 46%, 25% and 29% (Delhaye-Bouchaud et al., 1985) in the rat. The donkey PO was unfolded and occupied only the rostral half of the IOC (Fig. 3A, B) and similar to the rat, rabbit, pig, cat and squirrel monkey in its relative area and configuration (Kooy, 1916; Taber, 1961; Breazile, 1967; Gwyn et al. 1977; Rutherford and Gwyn, 1980; Azizi and Woodward, 1987; Bukowska et al., 2002).

In addition to the MAO, DAO and PO, there are four additional smaller subdivisions (the DC, nucleus β, VLO and DMCC) in most mammalian IOC. These cell groups were also observed in the donkey.

Together, with the rostral DC, the VLO is responsible for the generation of the vertical compensatory eye movements (Leonard et al., 1988; Graf et al., 1988), whereas the caudal DC is responsible for the horizontal movements. In the donkey, the DC and nucleus β appeared separated from each other (Fig. 3A). The VLO of the donkey IOC resembles that of rat, cat, rhesus monkey and rabbit, where it took the position of DC rostrally.

In the rat a dorsal extension develops from group c and then separates to form the DC, while the remaining dorsal extension of group c comprises the nucleus β (Flumerfelt and Hrycyshyn, 1986; Azizi and Woodward, 1987). In the rat, cat and rabbit, the DC elongates ventrolaterally to form the VLO (Taber, 1961; Bowman and Sladek, 1973; Brodal et al., 1975; Gwyn et al., 1977; Flumerfelt and Hrycyshyn, 1986; Azizi and Woodward, 1987; Bukowska et al., 2002). Moreover, the DC in the pig forms a connection between the MAO and the ventral lamella of PO (Breazile, 1967). In the donkey, both the DC and VLO were a discrete cluster of cells from first to last. The DC in the donkey was a very small group of cells, extending only a few sections in a rostrocaudal direction. The VLO in the donkey not only appeared laterally to the DC but also as a rostral extension of the DC. The vestibulocerebellum consists generally of the flocculonodular lobe and the ventral part of the uvula. The DC and VLO project into the vestibulocerebellum but are different in accurate

output and input. The DC has been divided into a rostral and caudal part (Graf et al., 1988; Leonard et al., 1988; Ruigrok, 2003). The rostral DC is more in line with the VLO (Tan et al., 1995; Sugihara and Shinoda, 2004; Voogd and Wylie, 2004). In the donkey the DC was very short in rostral to caudal representation so that it may be comparable to the caudal DC and the rostral DC in the donkey may be included into the VLO.

Generally the DMCC in most mammals appeared as isolated cell cluster dorsal to the main body (Taber, 1961; Breazile, 1967; Bowman and Sladek, 1973; Tan et al., 1995; Bukowska et al., 2002) except for monkey where it fuses rostrally with the ventral lamella of PO (Bowman and Sladek, 1973). According to Azizi and Woodward (1987), the DMCC disappears more caudally to the rostral end of the main body of MAO. In the donkey, as in the cat, pig, rabbit and rhesus monkey, the location of DMCC is similar to the description of Azizi and Woodward (1987) and does not form the most rostral structure of the MAO.

The four small cell groups, the DC, nucleus β, VLO and DMCC, have been considered as part of the MAO (Taber, 1961; Breazile, 1967; Bowman and Sladek, 1973; Rutherford and Gwyn, 1980; Azizi and Woodward, 1987). However, the other researchers considered that the DC and VLO are marked as belonging to the PO and the nucleus β and DMCC as belonging to the MAO (Kawamura and Hashikawa, 1970; Gwyn et al., 1977; Groenewegen et al., 1979; Brodal and Brodal, 1981; Tan et al., 1995; Ruigrok, 1997, 2003; Bukowska et al., 2002; Voogd and Wylie, 2004).

According to Ruigrok (2003) the nucleus β projects mainly into the nodules, and the DC and VLO project mainly into the flocculus, ventral paraflocculus and nodulus. The caudal DC projects only into the ventral paraflocculus and flocculus. The DMCC projects into the vermal uvula (Groenewegen et al., 1979). They consider the DC and VLO as parts of the PO. Azizi and Woodward (1987), who consider the four small cell groups as parts of the MAO, described that the vertical lamella of the MAO (group c and the four small cell groups) projects to the caudal vermis as well as the flocculus. Brodal and Brodal (1981) comment that the PO projects mainly into the lateral parts of the hemisphere, whereas the DC and VLO project to the flocculonodular lobe. Since the flocculonodular lobe are phylogenetically the oldest parts of the IOC, it may be questioned whether the DC and VLO should be considered as parts of the PO, which is the phylogenetically youngest part, or whether they should be considered to be a particular olivary subdivision. Thus, the classification of the four small cell groups could be not decided at the present moment. We made a diagram of the flattened and unfolded IOC as the four small cell groups to locate alongside the MAO.

The donkey IOC is totally similar to the most mammalian IOC except for the higher primate IOC in cytoarchitecture. Thus, we expect that, the donkey IOC may have a similar neural circuit to that of other mammals.

CHAPTER III

Morphologic characterization of the inferior olivary complex in the camel *(Camelus dromedarius)*

SUMMARY

The morphological structure of the inferior olivary complex (IOC) in the single humped camel (*Camelus dromedarius*) was investigated. Serial sections through the whole rostro - caudal extent of the IOC confirmed the configuration and interrelations of each compartment. The brain - stems from five fetuses of 600—800 mm crown—to—rump length (CRL) and a newborn camel were used in this study. The cytoarchitecture of the IOC was mapped in transverse serial sections, stained with toluidine blue or/and crystal violet. A descriptive nomenclature was adapted to a terminology that would imply analogy with other species. The IOC in the camel consisted of three major nuclei and four small cell groups. The medial accessory olivary nucleus (MAO) was the largest among the major nuclei; with its caudal half had a unique sickle—shaped configuration. In general the IOC in the camel showed a phyletic homology with other mammals.

INTRODUCTION

Camel is a hump−backed ruminant of the family Camelidae. and used as draft and saddle animals in desert regions of Africa, Arabia, and Asia. Adaptations to windblown deserts include double rows of eyelashes and the ability to close the nostrils.

The IOC works as a motor coordinator via projections to the cerebellum. The IOC is sole source of climbing fibers to the cerebellum (Sugihara et al, 1999). Axons arising from cells in the inferior olive cross and enter the inferior cerebellar peduncle to reach the contralateral cerebellar cortex. It is important to define the functional compartmentalization of the vermis and hemispheres (Groenewegen and Voogd, 1977; Sugihara et al, 2001). The compartmentalization in the olivocerebellar and olivonuclear projections seems to reflect a fundamental principle of input - output circuitry of the cerebellar system.

The aim of this study is to describe the morphology of the camel's IOC and to discuss its features in comparison with those in the IOC of the other mammals.

MATERIAL AND METHODS

The brainstems from five fetuses of 600－800 mm crown－to－rump length (CRL) and a newborn camel were removed and fixed in 10% formalin for at least three weeks. The brainstems were dehydrated and embedded in paraffin (2 cases) or/and in celloidin (4 cases). Serial sections were obtained at 50 μm thick from celloidin blocks and 10 μm thick from paraffin blocks, and were stained with toluidine blue or/and crystal violet. Series of line drawings of the IOC in the transverse plane were done. Each drawing will represent the approximate shape of the nucleus at the every respective point (Fig. 1).

The nuclei was described in topographical sequence from the caudal pole to the rostral pole of the IOC. Photos for the IOC were captured and cropped to an image processing application, to correct the brightness and contrast (Fig. 2).

RESULTS

The rostro-caudal length of the IOC was about 8-9 mm. Three major nuclei, MAO, DAO, and PO, as well as four small cell groups, were clearly detected in the camel IOC (Fig. 1, 2).

The MAO extended all over the total length of the IOC and disappeared a few sections before its rostral pole (Fig.1—31). At the caudal aspect of the MAO, three separate groups may be distinguished, labeled a, b, and c from laterally to medially (Fig. 2—A and B). Groups a and b appeared at the most-caudal levels, forming the caudal pole of the IOC. More rostrally, group c developed from group b medially. These three groups increased gradually in size and group c bent ventro-medially, thus the MAO assumed the shape of a sickle (Fig. 1 - 8). Nearly at the middle of IOC, a constriction separated group c from group b (Fig. 1-18). Group c rapidly disappeared (Fig. 1-20), while groups a and b merged each other to continue more rostrally (Fig. 1-31). The cytoarchitectural boundaries of groups a, b and c were rather clear in the caudal half of the MAO but obscure in the rostral half.

The DAO in the camel consisted of two lamellae; lateral and medial (LL and ML, respectively). The LL appeared medially as a round cell mass before the middle of the IOC, lateral to the DC and dorsal to the MAO (Fig. 1 - 14). The LL of DAO increased in size and shifted laterally to take its permanent position (Fig. 1 - 18). The ML of DAO appeared in the rostral half of IOC (Fig.1 - 20) and rapidly had a connection with the lateral lamella of DAO. Further rostrally the DAO extend as an horizontal sheet of cells and then it

curved ventro-laterally to connect with the dorsal lamella of PO (Fig. 1 - 28) followed by a connection with the ventral lamella of PO and then it disappeared just before the rostral pole of the IOC.

The PO in the camel consisted of two lamellae; dorsal lamella (*dl*) and ventral lamella (*vl*). The dl was the first lamella appeared as a group of cells between the ML of DAO and MAO (Fig.1 - 20). The *dl* of PO was larger than vl. The *vl* of PO appeared more rostrally and its medial end continued with DMCC. The two lamellae form a U shape with its hilus opened dorso—medially. More rostrally, dl was the first to get shorter, while *vl* appeared to be present at the same time with the DAO until the rostral pole.

Four small cell groups represented the dorsal cap of Kooy (DC), nucleus β, ventrolateral outgrowth (VLO) and the dorsomedial cell column (DMCC). DC appeared as a small mass of cells dorsal to group c (Fig. 1 - 7), and extended rostrally as a separate entity to the middle of IOC (Fig. 1 - 19). β nucleus appeared as a dorsal extension of the group c (Fig. 1 - 9), and continued dorsally with VLO in just rostral level (Fig. 1-10) . Further rostrally nucleus β separated from group c and shifted dorsally (Fig. 1 - 12). More rostrally, the nucleus β shifted ventrally to rejoin the subgroup c once again (Fig. 1 - 16). The nucleus β was never separated from the VLO until it disappeared around the middle of the IOC (Fig. 1—21). The VLO appeared as an isolated two cell masses, then coalesced and continued ventrally with the nucleus β (Fig. 1—10). More rostrally, the VLO increased in size and

pushed the DC laterally. The VLO disappeared at the same level with the nucleus β (Fig. 1−21). The DMCC appeared nearly at the beginning of the rostral one-fourth Of the IOC as a part of the medial side of the ventral lamella of the PO (Fig. 1−26). Slightly rostrally, DMCC appeared as a separate entity of cell cluster between the ventral lamella of the PO and the MAO and then disappeared (Fig. 1−28).

The IOC was imagined unfolded in one plane (Brodal et al., 1975) by pulling its compartments apart in the latero-medial direction (Fig. 3−A, B). The three dimensional construction of each nucleus was made using the transverse serial sections (Fig.4−A, B).

Figures and figure legends

Fig. 1 Line drawings of cross - section of the brainstem illustrating positions and relations among the nuclei of IOC in the camel. DAO; dorsal accessory olive, LL: lateral lamella of DAO, ML: medial lamella of DAO, MAO; medial accessory olive, PO; principal olive, a - c; groups a - c of the MAO, β; nucleus β, DC; dorsal cap, VLO; ventrolateral outgrowth, DMCC; dorsomedial cell column, dl; dorsal lamella of PO, vl; ventral lamella of PO.

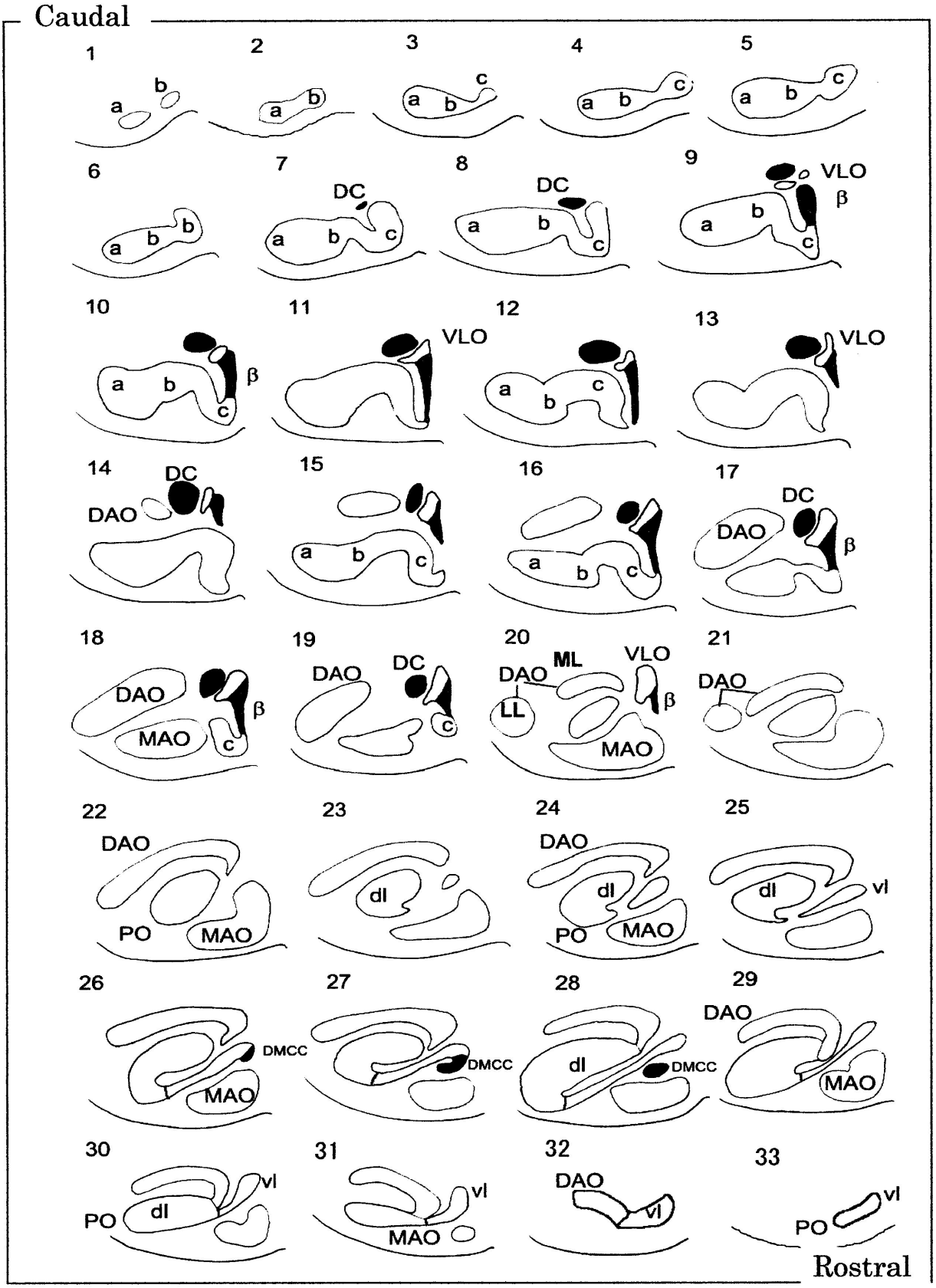
Caudal
1
2
3
4
5
6
7
8
9
10
11
12
13
14
15
16
17
18
19
20
21
22
23
24
25
26
27
28
29
30
31
32
33
a
b
c
DC
VLO
β
DAO
ML
LL
MAO
PO
dl
vl
DMCC
Rostral

Fig. 1

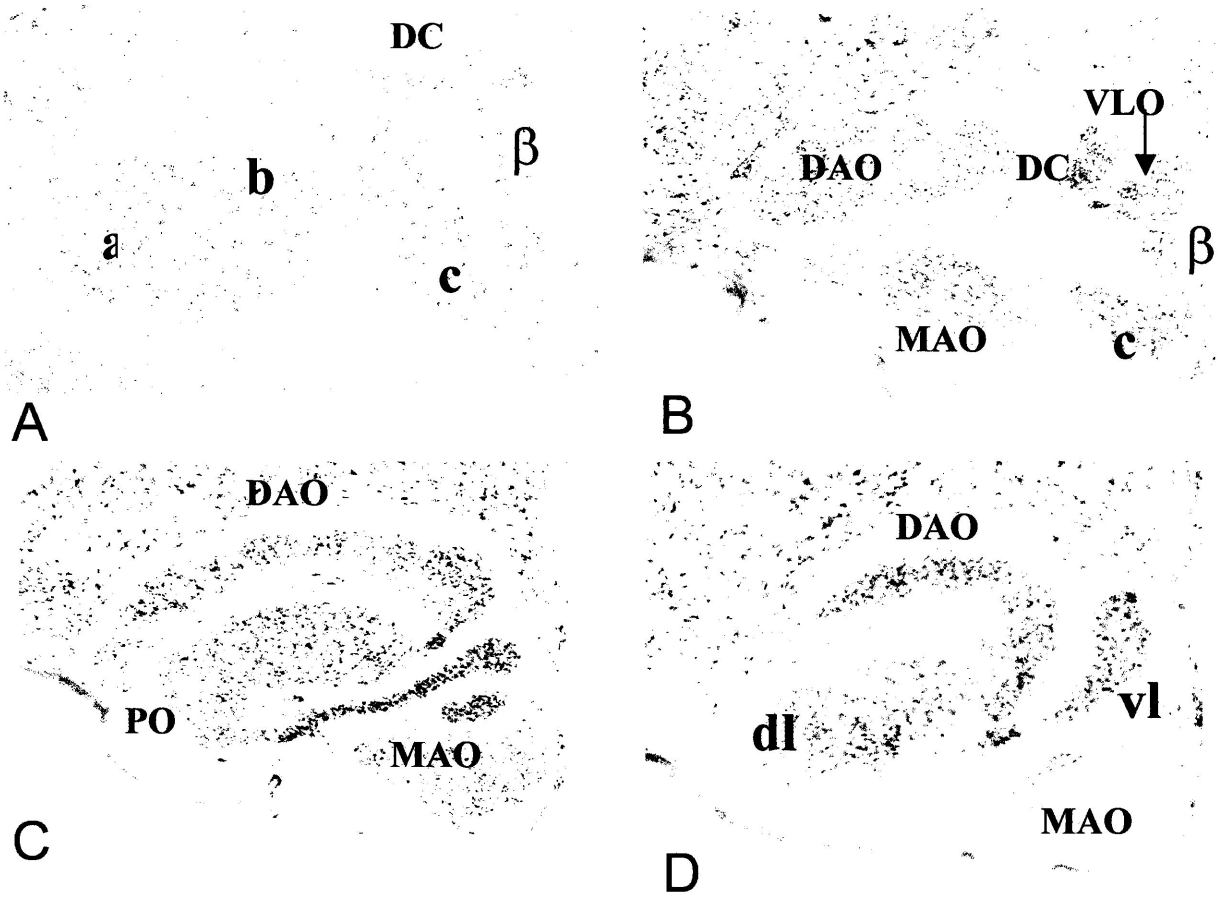

Fig.2

Light micrographs of transverse section of the IOC. (A) Light micrograph illustrating the Sickle-shaped MAO. (B) Light micrograph illustrating the division of the MAO. (C) Light micrograph illustrating the major nuclei of the IOC. (D) Light micrograph IOC in the camel before its rostral pole. (A) corresponds to Fig.1-8, (B) to Fig. 1- 18, (C) to Fig. 1- 28 and (D) corresponds to Fig. 1-30

Fig. 3 A and B Summarizing diagram of the imagined unfolded IOC.

See Fig. 1 for abbreviations.

R: rostral, C: caudal, M: medial, L: lateral

Fig. 4 A and B Three-dimensional Model of MAO, PO, and DAO in the camel IOC. See Fig. 1 for abbreviations.

R: rostral, C: caudal, M: medial, L: lateral

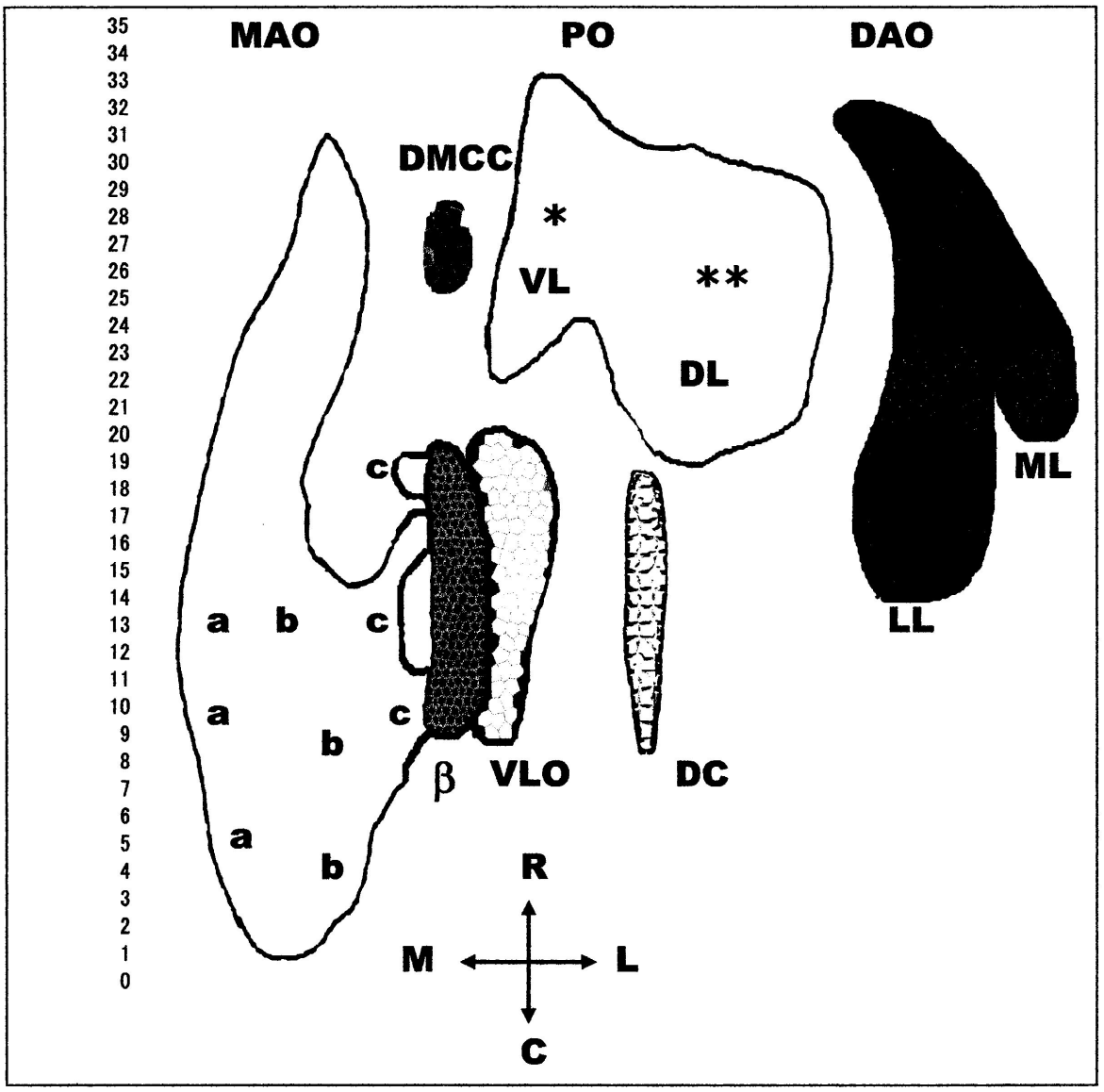
35
34
33
32
31
30
29
28
27
26
25
24
23
22
21
20
19
18
17
16
15
14
13
12
11
10
9
8
7
6
5
4
3
2
1
0
MAO
PO
DAO
DMCC
*
VL
**
DL
ML
LL
c
a
b
c
a
c
b
a
b
β
VLO
DC
R
M
L
C

Ⓐ

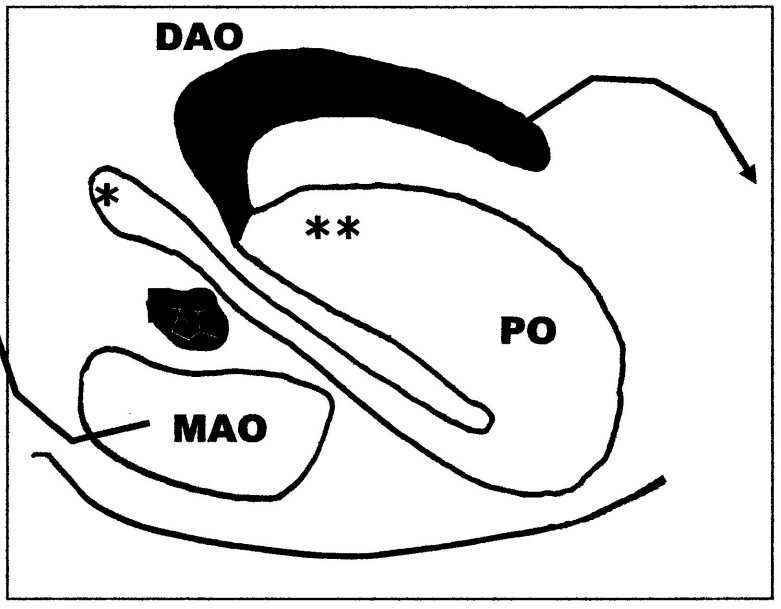
DAO
*
**
PO
MAO

Ⓑ

Fig. 3

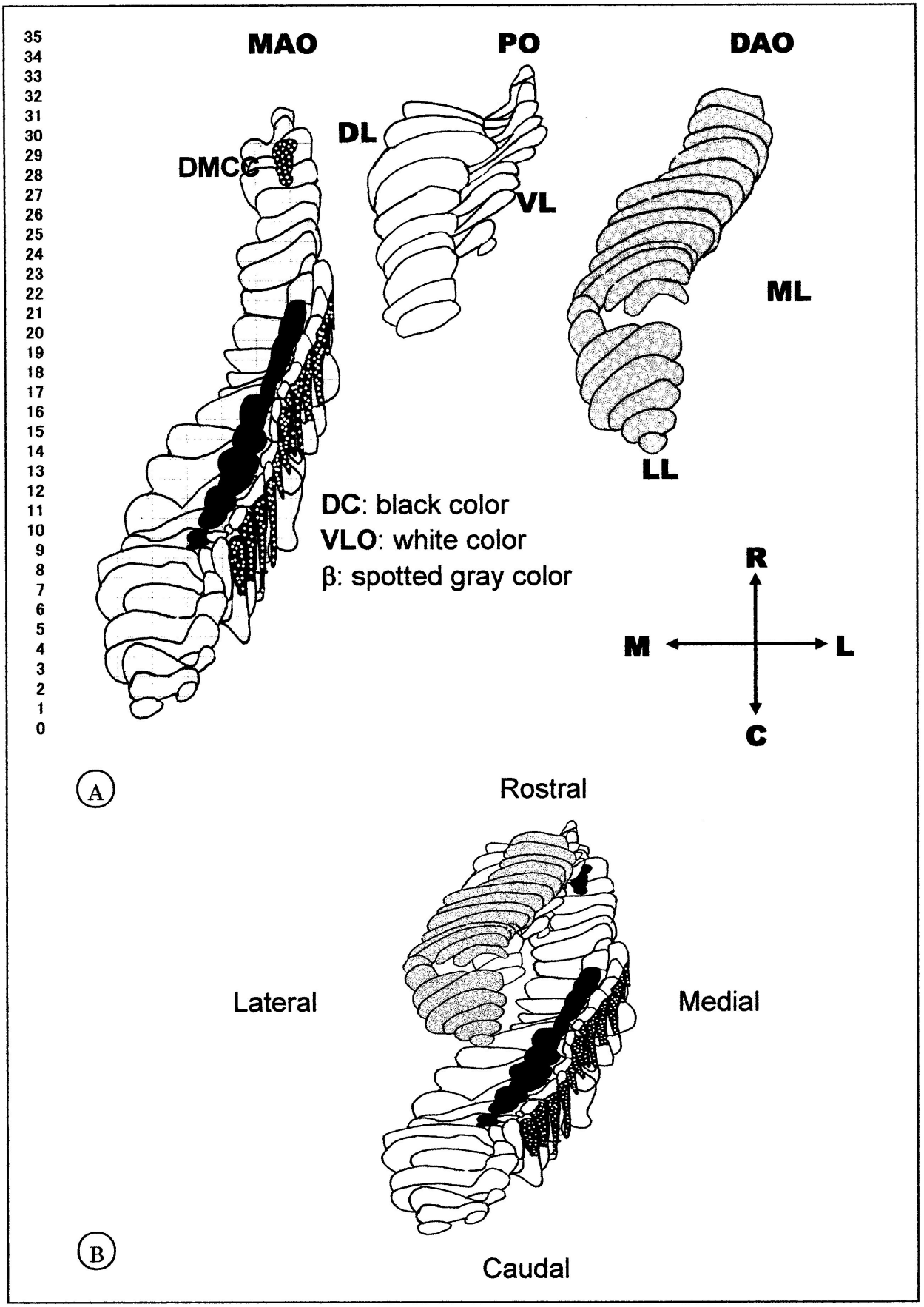
35
34
33
32
31
30
29
28
27
26
25
24
23
22
21
20
19
18
17
16
15
14
13
12
11
10
9
8
7
6
5
4
3
2
1
0
MAO
PO
DAO
DMCC
DL
VL
ML
LL
DC: black color
VLO: white color
β: spotted gray color
R
M
L
C
A
Rostral
Lateral
Medial
Caudal
B

Fig.4

DISCUSSION

The mammalian IOC is divided generally into three major nuclei and four small cell groups (Kooy, 1916; Azizi and Woodward, 1987). The general conformation of IOC of the camel as described in this study did as well.

In most mammals except for the primates, MAO is the largest of the three main nuclei of the IOC (Moatamed, 1968; Armstrong, 1974; Azizi and Woodward, 1987). According to Ruigrok and Voogd (2000), in the rat, the MAO is usually divided into the rostral and caudal halves. At the caudal aspect of the MAO three separate groups may be distinguished, labeled a, b, and c from laterally to medially (Whitworth & Haines, 1986). At the caudal most levels, the nucleus β is located medially but, upon advancing rostralward, it takes up a more dorsal position relative to group c Azizi and Woodward, 1987). In the camel, the MAO resembled that of other mammals but the sickle shape of a, b and c groups was different from other mammals, which take the form of an horizontal lamella. The nucleus β in camel appeared as the dorsomedial angle of the sickle - shaped MAO. Slightly rostrally, the nucleus β was continued dorsally with the VLO and ventrally with group c.

According to Voogd and Ruigrok (2004), the DMCC with its bilateral and branching projections (Sugihara et al, 1999) to the lateral P3+ and the P4+ bands of the caudal vermis (Voogd et al, 1996) should be considered as a separate subnucleus of the IOC. In most mammals, the DMCC appeared as isolated cell cluster dorsal to the MAO (Taber, 1961; Breazile, 1967; Bowman

and Sladek, 1973; Tan et al, 1995; Bukowska et al., 2002). According to Azizi and Woodward (1987), the DMCC in the rat start as isolated cell cluster and more rostrally, DMCC fuses with the medial part of the *vl* of PO (Gwyn et al, 1977; Azizi and Woodward 1987). While in the pig, the DMCC is much reduced and has no continuity with other cell groups (Breazile, 1967). The DMCC in the camel appeared initially continuous with the *vl* of PO, further rostrally, detached from the *vl*; this course of the DMCC was much similar to the DMCC of the rhesus monkey (Bowman and Sladek, 1973).

The DAO is generally the smallest nucleus of the IOC and consists of one lamella, except for the rat, where it consists of two lamellae joined laterally (Schild, 1970; Delhaye - Bouchaud et al, 1985; Azizi and Woodward, 1987)). The DAO in the pig, goat, and horse start medially then moves laterally and then relocated medially (Kooy, 1916). The medial side of DAO is continuous with the *dl* of PO, and more rostrally becomes continuous with the *vl* of PO (Kooy, 1916; Brodal et al, 1975). In the pig, this configuration is reversed (Breazile, 1967), and in the sheep DAO has no connection with the PO (Saigal et al., 1983). The DAO in the camel consisted of two lamellae; the LL which started more caudally than the ML and then the two lamellae united together forming one lamella, which arched over the PO and MAO. Rostrally to level 22 (Fig. 1) the DAO continued as a single lamella joined medially with the *dl* of the PO.

The PO has much the same shape in all mammals except for the higher primates (Kooy, 1916). PO consists of *dl* and *vl*, joined at their lateral bend.

Moreover, the ventrolateral outgrowth (VLO) and dorsal cap of Kooy (DC) are usually considered as a caudal continuation of the PO (Brodal and Kawamura, 1980; Ruigrok and Cella, 1995; Ruigrok and Voogd, 2000). The PO is the smallest nucleus in the rodent IOC and the largest in the human IOC (Moatamed, 1968; Armstrong, 1974; Azizi and Woodward, 1987). In primates, the PO is well developed with many folds (Kappers et al, 1960; Bowman and Sladek, 1973). Numerical studies show that the MAO, DAO and PO contain neurons at proportions of 10%, 4% and 86%, respectively, in humans (Moatamed, 1968) and 49%, 24% and 27%, in rat (Schild, 1970) or 46%, 25% 29% (Delhaye - Bouchaud et al, 1985). The PO in the camel PO had no flexure and consisted of two lamellae; *dl*, which was larger than the *vl* (Fig. 2 - C). Generally, the PO of the camel was similar to many mammals except for the higher primates, in its relative area and configuration (Kooy, 1916; Taber, 1961; Breazile, 1967; Schild, 1970; Gwyn et al, 1977; Rutherford and Gwyn, 1980; Azizi and Woodward, 1987; Bukowska et al, 2002).

According to Azizi and Woodward (1987), in the rat a dorsal extension develops from group c and then separates to form the DC, while the remaining dorsal extension of group c comprises the nucleus β. In the rat, cat, rhesus monkey and rabbit, the DC elongates ventrolaterally at rostral levels and becomes the VLO (Bowman and Sladek, 1973; Brodal et al, 1975; Flumerfelt and Hrycyshyn, 1986; Azizi and Woodward, 1987; Bukowska et al, 2002). Moreover, the DC in the pig forms a connection between the MAO and the ventral lamella of PO (Breazile, 1967). Together with the rostral DC

(rDC), the VLO is responsible for the generation of the vertical compensatory eye movements (Leonard et al, 1988; Graf et al, 1988), whereas the caudal Dc (cDC) is responsible for the horizontal movements. In the camel, the DC appeared as an isolated cell cluster over the MAO and never had a connection with any other nuclei. The VLO in the camel appeared caudally as an isolated small cell clusters which coalesce and joined the nucleus β.

The cerebellar cortex is classically and functionally divided into the vermis, paravermis (intermediate zone), and lateral hemispheres (Voogd and Glickstein, 1998; Voogd and Ruigrok, 2004). These three broad zones are subdivided into seven longitudinal sub-zones, each of its particular climbing fibers afferent from subnucli of the IOC. Vermal zones A and X receives mainly projection from the caudal MAO (group a−c) and vermal zone B from the caudal DAO. Paravermal zones C_1, C_2, and C_3 are innervated by the rostral main part of the MAO and the rostral DAO respectively, and the hemisphere from the PO. The D zones of the hemispheres receive climbing fibers from the PO. The DC and VLO innervate the nodulus and flocculus of the vestibulo−cerebellum; the group b and the DMCC project to the nodulus and the uvula (Flumerfelt and Hrycyshyn, 1986; Azizi and Woodward, 1987).

The basic topography of the olivary projection to the CN in the rat resembles the organization observed in the cat based on retrograde (Dietrichs and Walberg, 1989) and anterograde tracer studies (Courville, 1975; Groenewegen and Voogd, 1977; Groenewegen et al, 1979; Ruigrok and Voogd,

2000), it was shown that the caudal half of the MAO is connected to the fastigial nucleus, which is the equivalent of the MCN in the rat. The PO was shown to project to the dentate nucleus (LCN) and the rostral halves of both accessory olives were connected to the interposed nuclei.

In this paper, we conclude that the IOC in the camel resembles that of other mammals except for the higher primates, as well in its principal lines, as in many details. The IOC of the camel, horse, goat, cat, rodent and rabbit showed a phyletic continuity within these species (Butler and Hodos, 2005). It is suggested that the olivocerebellar and olivonuclear projections of camel IOC probably are similar to that of these species.

Chapter IV

A quantitative study of Purkinje cells and inferior olive neurons in the chicken

SUMMARY

A single olivocerebellar fiber branches off several climbing fibers. One Purkinje cell receives input from only one climbing fiber. A single inferior olivary neuron, therefore, synapses with several Purkinje cells so that there are more Purkinje cells than the inferior olivary neurons. We aimed to elucidate the numerical ratio of the inferior olivary neurons to Purkinje cells in the chicken. The total numbers were 353,834 ± 5,274 Purkinje cells per the cerebellum and 21,553 ± 904 inferior olivary neurons of both sides. The numerical ratio of inferior olivary neurons to Purkinje cells was 1:16. The ratio of those neurons in mammals is about 1:4-17 so that the ratio in the chicken is within the range of mammals.

INTRODUCTION

The mammalian inferior olivary complex (IOC) consists basically of the medial and dorsal accessory olivary nuclei (MAO and DAO, respectively), and the principal olivary nucleus (PO). The accessory nuclei are older than the PO and the MAO is the oldest in phylogenetic viewpoint (Kuhlenbeck, 1975). The avian IOC consists of a large dorsal and a small ventral lamellae. It has been believed on the basis of the morphological appearance that the ventral lamella corresponds to the PO, the lateral and medial parts of the dorsal lamella are the homologue of the DAO and MAO, respectively (Kuhlenbeck, 1975). Recently, it is suggested that the chicken dorsal lamella represent the DAO, PO, and the rostral and a small part of the caudal MAO, while the ventral lamella represents most of the caudal MAO on the basis of the olivocerebellar projection (Furber, 1983).

Purkinje cells (PCs) are known to receive double inputs from the mossy and climbing fibers. An olivocerebellar fiber gives off several climbing fibers, but each Purkinje cell receives only one climbing fiber (Eccles et al., 1966). The IOC is the sole source of the climbing fibers in birds and mammals (Brodal et al., 1950; Freedman et al., 1977). Although there are several quantitative studies on the PCs and the IOC neurons, there are a few studies on a numerical correlation between PC and IOC neurons by the same researcher. Our goal of this study is to elucidate the numerical ratio of the IOC neurons to PCs in the chicken.

MATERIALS AND METHODS

Seven chickens (*Gallus domesticus*) (four males and three females) ranging from 1.5 to 2 months of age (300 to 500 g in body weight) were used in this study. The animals were deeply anesthetized with sodium pentobarbital (Nembutal). After intravenous administration of heparin (270 IU) the animals were perfused with 800 m*l* of 0.75% saline, followed by 800 m*l* of 10% formalin through the left ventricle. Both solutions were delivered at 70 m*l*/min (Freedman et al., 1977). After two to three hours of perfusion, the brain was removed. The specimens were dehydrated, embedded in celloidin, and were serially cut at 30 μm and stained with toluidine blue or thionin. The medulla was sectioned transversely while the cerebellum was sectioned sagittally. Cell counts were done by projecting the microscopic sections onto an Olympus Video Micro Meter [Model VM-31] at final magnification x 350. In four chickens, the IOC neurons of both sides were counted in every fifth section. The procedure was repeated on three separate occasions.

RESULTS

The total number of the IOC neurons was then estimated by multiplying the number of neurons counted by 2 (2 is half of the number of sections non-counted between the section counted and the next counted section) (Escobar et al., 1968). All visible neurons with and without a nucleolus were included in the counts. To check the reliability of this method, we counted only the neurons with a nucleolus in two successive sections of one case, and then compared for both methods. The two methods gave no significant differences in the total cell number.

PCs with a nucleolus were counted in every tenth section in the other three chickens. The total number of PCs in the cerebellum was obtained by multiplying the number of PCs counted by 10 (Mlonyeni, 1973).

The left and right IOC included 10,733 and 10,820 neurons, respectively, and therefore, there were 21,553 IOC neurons on average in both sides (Table 1). There were no significant differences between the left and right sides and even in sexual difference.

The number of IOC neurons of the dorsal lamella was about three times greater than of the ventral one, representing 74.4% of the total number of the IOC neurons, and the lateral part (48.2%) contained more neurons than the medial part (26.2%).

Table 1. Counts of inferior olive neurons in the chicken

	Dorsal Lamella		Ventral Lamella	TOTAL
	16,036			
	74%			
	L	M		
Average	10,397	5,639	5,517	21,553
Percent	48%	26%	26%	100%
SD	933	503	710	904
CV	9.1%	8.9%	13.0%	4.2%

SD, standard deviations.

CV, coefficient of variation.

L & M, the lateral and medial part of the dorsal lamella.

Table 2. Purkinje cell numbers in each lobule of chicken cerebellum

	I	II	III	IV	V	VI	VII	VIII	IX	X	TOTAL
Average	9,269	17,665	22,070	23,137	49,170	47,437	39,061	51,603	77,063	17,358	353,834
Percent	2.6%	5%	6.24%	6.5%	13.9%	13.4%	11%	14.6%	21.8%	5%	100%
SD	275	1,331	1,728	457	4,688	967	1,355	2,028	3,910	1,240	5,275
CV	3.0%	7.5%	7.8%	2%	9.5%	2%	3.5%	3.9%	5.1%	7.1%	1.5%

SDEV, standard deviations.

CV, coefficient of variation.

I-X, the number of the chicken cerebellar folia.

DISCUSSION

In the previous study, the dorsal lamella is markedly larger than the ventral one and the lateral part is the largest component of the dorsal lamella (Voogd-Nilson, 1954), and the dorsal and ventral lamellae contain about 75% and 25% of the total number of IOC neurons, respectively (Lopez-Roman and Armengol, 1996). Thus, our present results agree with those of the previous studies.

The avian cerebellum consists exclusively of the vermis on the basis of gross anatomy. However, the lateral parts of lobules VI - VIII has been considered to correspond to the cerebellar hemispheres, which receive the most abundant input from the pontine nuclei (Brodal et al., 1950; Whitlock, 1952; Dubbeldam, 1998). In the mammalian IOC, the MAO, DAO and PO project generally into the vermal and paravermal zones and the hemisphere, respectively. Thus, it is expected that in the chicken IOC the MAO is largest and PO is smallest. Contrary to our expectation the DAO (namely, the dorsal lamella) in the classical interpretations was largest and the MAO was similar in neuronal number to the PO in this study. The subdivisions of the chicken IOC that are suggested by Furber (1983) in term of the olivocerebellar projection, however, are suitable for this study.

The avian cerebellum consisted of 10 lobules. The number of PCs was 353,834 on average. The numbers were highest in the lobule IX (21.8%) and lowest in the lobule I (2.6%) (Table 2).

In this study IOC neurons were about 21,600 and PCs were about 354,000 in the total average numbers. The ratio of the former to the latter, therefore, was

about 1:16. In the previous studies, the chick IOC neurons in both sides are 14,350 (Lopez-Roman and Armengol, 1996) or about 14,000 (Armstrong and Clarke, 1979) in number. The number of PCs is 262,000 (Armstrong and Clarke, 1979). The ratio of both, therefore, is about 1:18, that is similar to our result.

The total numbers of IOC neurons have been estimated in the human, vampire bat, cat and rat. These were about 909,000 (Harvey and Napper, 1988) or 1,102,000 in the human (Moatamed, 1968], 26,000 in the vampire bat (Escobar et al., 1968) 140,000 (Escobar et al., 1968) or 151,000 (Mlonyeni, 1973) in the cat, and 49,000 (Schild, 1970) or 57,000 (Delhaye—Bouchaud et al., 1985) in the rat. Although the avian IOC conspicuously developed in correlation with the expanded cerebellum (Kuhlenbeck, 1975), the chicken IOC neurons are much fewer than in lower mammals, such as the vampire bat and the rat.

The total numbers of PCs are estimated in several mammals, including the human, cat and rat. These are about 15 million in the human (Nairn et al., 1989; Mayhew et al., 1990; Mwamengele et al., 1993), 1,440,000 to 1,809,000 in the cat (Mlonyeni, 1973; Mwamengele et al., 1993), and 254,000 to 360,000 in the rat (Armstrong and Schild, 1970; Harvey and Napper, 1988; Mwamengele et al., 1993). The chicken cerebellum has as many PCs as the rat, unlike with the number of IOC neurons.

From the above mentioned data the estimated numerical ratio of IOC neurons to PCs is about 1:15-17 in the human, 1:10-13 in the cat and 1:4-7 in

the rat. According to Sugihara et al. (2001) who observed the complete trajectories of the single olivocerebellar fiber, the single fiber branches off seven climbing fibers on average in the rat. Their result nearly corresponds to the above described data on the rat. Therefore, the numerical ratio of IOC neurons to PCs in the chicken falls within the range of mammals. It is suggested that the chicken olivocerebellar system works with the same principle as mammalian one.

GENERAL CONCLUSION

In the chapter I, II, and III, the inferior olivary complex (IOC) was morphologically studied in three different species of large mammals (the water buffalo, donkey and camel, respectively).

Recently, neural circuits were precisely analyzed using many neuronal tracers including HRP, WGA-HRP, BDA and so on. It has been made known that each region of the IOC projects into specific regions in the cerebellar cortex and cerebellar nuclei. However, these new methods with neuronal tracers are applied to small experimental animals but not to the large animals. In this study, I intended to observe the morphology of the IOC of large animals and to compare our results with the IOC in the experimental animals.

The IOC was generally composed of three major nuclei (medial and dorsal accessory olivary nuclei, MAO and DAO, and a principal olivary nucleus, PO) and four small cell groups.

The MAO was the largest among the major nuclei but the MAO of the water buffalo is relatively short among the three animals. The main part of the MAO consists a, b and c cell groups, with its caudal half formed an horizontal lamella in water buffalo, a sickle shape in camel and an S shape in the donkey.

The DAO was boomerang-shaped structure consisted of one lamella with its medial part had a connection with the dorsal lamella of PO. Caudal to the rostral pole of the IOC, the DAO lost its connection the dorsal lamella of the PO and formed a connection with the ventral lamella

of the PO. The DAO in the donkey is relatively long in rostrocaudal direction. However, its caudal part is sparse in neuronal density with unclear outline. Thus, the neuronal number of the donkey DAO probably is less numerous than the MAO or PO.

The PO was a simple U-shaped structure consisted of dorsal and ventral lamellae, which are joined at their lateral bend. Both lamellae were equal in size in donkey while in the water buffalo and camel the dorsal lamella was larger than the ventral lamella.

The four small cell groups, the dorsal cap (DC), nucleus β, ventrolateral outgrowth (VLO) and the dorsomedial cell column (DMCC), were morphologically similar among the three animals and matched the previous reports (for example, Armstrong, 1974) in their relative position and orientation. However, the DC and VLO were different in development among the three animals. The DC and VLO were relatively small in the donkey and well developed in the water buffalo and camel.

We conclude that the IOC in the water buffalo, donkey and camel showed a phyletic continuity with other mammalian species except for the higher primates (Butler & Hodos, 2005). Consequently, the olivocerebellar and olivonuclear projections of the IOC of water buffalo, donkey and camel probably will be similar to that of these species.

In the chapter III and IV, the IOC neurons and Purkinje cells were morphometricaly examined in the water buffalo and chicken. In the water buffalo, the total number of neurons on both sides of the IOC was 211,000±7,000 cells. The average neuron density was 3,000 cell / mm^3.

The ratio between the Purkinje cells and IOC neurons in mammals is about 1:14-17. Thus it was possible to estimate the number of Purkinje cells by the neuronal number of the IOC.

In the chicken, the total numbers were 353,834±5,274 in the Purkinje cells per cerebellum and 21,553±904 in the IOC neurons of both sides. The numerical ratio of IOC neurons to Purkinje cells was 1:16. The ratio in the chicken is within the range of mammals.

Japanese Summary: 論文要旨

第 1-3 章において、三種の大型哺乳類（スイギュウ *Buballus bubalis*、ロバ *Equus asinus* およびヒトコブラクダ *Camelus dromedarius*）のオリーブ核（IOC）を形態学的に観察した。近年、HRP を初めとして多くのレクチンやデキストランアミンなどの神経標識物質の発展により神経回路は極めて詳細に解析できるようになった。IOC についても、IOC の各部位は小脳皮質、および小脳核の特定の部位に投射することがますます明らかになってきた。しかし、これら標識物質を用いた研究は経費との関係などから実験動物に適用されるものがほとんどであり、とりわけ大型動物や野生動物に関しての報告はほぼ見られない。そこで、大型動物では実験動物で得られた結果を参考にして、細胞構築学的研究を見直すことによって、これら大型動物の神経回路網を推測することが求められている。本研究では、家畜でありながら今まで研究が進んでいない大型動物としてスイギュウ、ロバおよびヒトコブラクダの IOC の連続切片を作製して、詳細にその構造を観察することを目的とした。

三種の IOC はすべて三つの核、すなわち内側および背側副オリーブ核（MAO, DAO）と主オリーブ核（PO）、と四つの小細胞群、dorsal cap (DC), ventrolateral outgrowth (VLO), nucleus β, dorsomedial cell column (DMCC)、から構成されていた。MAO は三核中で最大の核であった。MAO は IOC の尾端を構成し、ほぼ IOC 全長に渡って伸張していたが、三種の中ではスイギュウの MAO は DAO より頭尾方向に若干長い程度であり、DMCC が MAO の頭側に位置していた。他の二種の DMCC は MAO の頭端よりやや尾側を占めていた。MAO 主部の尾側部は a, b, c の３細胞群を区別し、これらによってスイギュウでは水平な平板状、ヒトコブラクダでは鎌状、そしてロバではＳ字状を呈していた。DAO は IOC の頭側 60-80%を占め、ロバでは IOC の頭端を、他の２種では PO が DAO よりわずかに頭側に伸張していた。この中でロバの DAO は最も頭尾方向に長い上に、尾側部は細胞密度が低く、輪郭が曖昧な領域を含んでいた。従ってロバの DAO は比較的大きく見えても細胞数が多いわけではなかった。DAO は全体にブーメラン状をし、その

中間部でPOの背側層板と結合し、頭端のやや尾側では背側層板と離れて、腹側層板と結合した。

POはすべての動物でIOCの頭側半分以内にあって、横断面では背側と腹側層板からなる単純なU字状を呈していた。ヒトなどの高等霊長類のPOは三つの核中で最も大きく、多くのヒダを作っているが、今回の三種はラットやネコと同様に屈曲は単純であった。二つの層板はほぼ同大であったがヒトコブラクダでは背側が大きかった。

四つの小細胞群はその相対的位置関係や方向において他の多くの哺乳動物と類似し、今回の三種の動物間でも類似していた。ただし、DCとVLOの発達程度には差が見られ、ロバではDCが小さい上に両細胞群の境界がはっきりせず、あたかも一つの細胞群のように見え、ヒトコブラクダでは最もよく発達していた。以上、IOCの構造的特徴は良く研究されているラットやネコと基本的に類似しており、ヒトなどの高等霊長類のIOCが哺乳類全体から見ると特別な存在であると言える。

小脳には登上線維と苔状線維が終止しているが、登上線維は唯一IOCに起始している。IOCニューロンのほぼすべてがオリーブ小脳路線維であり、オリーブ小脳路線維は小脳核に側副枝を出した後に数本の登上線維に分岐し、各登上線維はプルキンエ細胞の樹状突起と1対1の関係で終止している。第1章ではスイギュウのIOCニューロン数を、第4章ではIOCニューロンとプルキンエ細胞数を算定した。スイギュウのIOCニューロンは両側を合算して約21万個、平均密度は約3千個/立方ミリであった。哺乳類におけるIOCニューロン数とプルキンエ細胞の比率は1：4-17と言われていることから、プルキンエ細胞数も大方予想できる。

第4章において、ニワトリのIOCニューロンとプルキンエ細胞の総数を算定した。その結果、ニワトリのIOCニューロンとプルキンエ細胞の比率は1：16であり、この値は哺乳類で報告されている範囲内であった。鳥類のIOCは背腹の二葉からなり、小脳は小脳半球を欠いていることから哺乳類のIOCおよび小脳と構造的に大きく異なっている。しかし、今回の結果は、鳥類の登上線維と小脳の関係は基本的に哺乳類のそれと同じであると言われていることを支持するものといえる。

ACKNOWLEDGMENTS

The research for this PhD-thesis was carried out at Department of Veterinary Anatomy, Faculty of Agriculture, Tottori University. My sincere appreciation and gratitude belong to my supervisor Professor Dr. **Masato Uehara** (Tottori University) for his firm guidance and sensible touch throughout this work. I am deeply grateful to my co-supervisor Associate Professor Dr. **Tomohiro Imagawa,** for sharing his amazing scientific insight, and for his dedication and encouragement during this work. I also wish to thank my co-supervisor Professor Dr. **Kiso Yasuo** (Yamaguchi University). Additional thanks belong to D.V.M. **Suzuki Jun** and D.V.M. **Shinozaki Aya** (Tottori University). I also want to thank all the other co-authors for their contributions in this work. I am also grateful to all students of Department of Veterinary Anatomy, Tottori University for their continuous support and assistance.

My sincere appreciation and gratitude belong to my Professor Dr. **Ashraf S. Saber** and my Professor Dr. **Atef M. Erasha** and all my colleagues in Department of Veterinary Anatomy, Menufiya University (Egypt) for the unconditional support I received from them.

Finally, I am especially grateful to my family for their endless love, the encouragement given to me, and for supporting me.

REFERENCES

Armstrong, D.M. 1974. Functional significance of connections of the inferior olive. *Physiol. Rev.*, 54, 358−417.

Armstrong, D.M. and Schild, R.F. 1970. A qualitative study of the Purkinje cells in the cerebellum of the albino rat. *J. Comp. Neurol.,* 139, 449−456.

Armstrong, R.C. and Clarke, P.G.H. 1979. Neuronal death and the development of the pontine nuclei and inferior olive in the chick. *Neuroscience,* 4, 1635 - 1647.

Azizi, A.S. and Woodward, D.J. 1987. Inferior olivary nuclear complex of the rat: morphology and comments on the principles of organization within the olivocerebellar system. *J. Comp. Neurol.*, 263, 467−484.

Bowman, J.P. and Sladek, J.R. 1973. Morphology of the inferior olivary complex of the rhesus monkey (*Macaca mulatta*). *J. Comp. Neurol.,* 152, 299 - 316.

Bowman, M.H. and King, J.S. 1973. The conformation, cytology and

synaptology of the opossum inferior olive nucleus. *J. Comp. Neurol.*, 148, 491−524.

Bozhilova - Pasirova, A. and Ovtscharoff, W. 2000. The inferior olivary complex. *Adv. Anat. Embryol cell Biol. Review,* 155, III - VI, 1 - 84.

Breazile, J.E. 1967. The cytoarchitecture of the brain stem of the domestic pig. *J. Comp. Neurol.,* 129, 169 - 188.

Brodal, A. 1940. Experimentelle Untersuchungen uber die olivo-cerebellare Lokalisation. *Z. Ges. Neurol. Psychiat.*, 169, 1 - 153.

Brodal, A. and Kawamura, K. 1980. Olivocerebellar projection: a review. *Adv. Anat. Embryol. Cell Boil., 64,* 1 - 140.

Brodal, A., Kristiansen, K. and Jansen, J. 1950. Experimental demonstration of a pontine homologue in birds. *J. Comp. Neurol.*, 92, 23 - 70.

Brodal, A., Walberg, F. and Hoddevik, G.H. 1975. The olivocerebellar projection in the cat studied with the method of retrograde axonal transport of horseradish peroxidase. *J. Comp. Neurol.,* 164, 449 - 470.

Brodal, P., Brodal, A., 1981. The olivocerebellar projection in the monkey.

Experimental studies with the method of retrograde tracing of horseradish peroxidase. *J Comp Neurol.,* 201, 375-93.

Bukowska, D., Zguczynski, L. and Mierejewska-Krzyzowska, B. 2002. Axonal collateral branching of neurons in the inferior olive projecting to the cerebellar paramedian lobule in the rabbit. *Cells Tissues Organs,* 172, 37−47.

Butler, A.B. and Hodos, W. 2005. Evolution and the organization of the central nervous system. In: Comparative vertebrate neuroanatomy. *John Wiley and Sons, Hoboken.* pp, 2923.

Courville J. 1975. Distribution of olivocerebellar fibers demonstrated by a radioautographic tracing method. *Brain Res.*, 95, 253−263.

De Zeeuw, C.I., Simpson, J.I., Hoogenraad, C.C., Galjart, N., Koekkoek, S.K.E., and Ruigrok, T.J.H, 1998. Microcircuitry and function of the inferior olive. *Trends Neurosci.,* 21, 391−400.

Delhaye-Bouchaud, N., Geoffroy, B. and Mariani, J. 1985. Neuronal death and synapse elimination in the olivocerebellar system. I. Cell counts in the inferior olive of developing rats. *J. Comp. Neurol.*, 232, 299−308.

Desclin, J.C. 1974. Histological evidence supporting the inferior olive as

the major source of cerebellar climbing fibers in the rat. *Brain Res.,* 77, 365−384.

Dubbeldam, J.L. 1998. pp. 1525-1636. *In:* The Central Nervous System of the Vertebrates, vol. 3 (Nieuwenhuys, R., Ten Donkelaar, H.J. and Nicholson, C. eds.), Springer, Berlin.

Eccles, J.C., Llinas, R. and Sasaki, K. 1966. The excitatory synaptic action of climbing fibers on the Purkinje cells of the cerebellum. *J. Physiol.,* 182, 268 −296.

Escobar, A., Sampedro, E.D. and Dow, R.S. 1968. Quantitative data on the inferior olivary nucleus in man, cat and vampire bat. *J. Comp. Neurol.,* 132, 397−400.

Farhad, M. 1966. Cell frequencies in the human inferior olivary nuclear complex. *J. Comp. Neurol.,* 128, 109−116.

Flumerfelt, B.A. and Hrycyshyn, A.W. 1986. Precerebellar nuclei and red nucleus. In: Paxinos, G. (Ed.), The Rat Nervous System, *Academic Press, New York (1985),* vol. 1. pp, 229−237.

Freedman, S.L., Voogd, J. and Vielvoye, G.J. 1977. Experimental

evidence for climbing fibers in the avian cerebellum. *J Comp Neurol.,* 175, 243−252.

Furber, S.E. 1983. The organization of the olivocerebellar projection in the chicken. *Brain Behav. Evol.*, 22,198−211.

Futami, K. and Okamoto, M. 1968. Anatomy of the olivary nucleus and surrounding areas. *Advan. Neurol. Sci. Tokyo,* 12, 341−367.

Graf, W, Simpson, J.I. and Leonard C.S. 1988. Spatial organization of visual messages of the rabbit's cerebellar flocculus. II. Complex and simple spike response to Purkinje cells. *J. Neurophysiol.,* 60, 2091−2121.

Groenewegen, H.J. and Voogd, J. 1977. The parasagittal zonation within the olivocerebellar projection; I. Climbing fibers distribution in the vermis of cat cerebellum. *J. Comp. Neurol.,* 174, 417−488.

Groenewegen, H.J., Voogd, J. and Freedman, S.L. 1979. The parasagittal zonation within the olivocerebellar projection; II. Climbing fibers distribution in the intermediate and hemispheric parts of cat cerebellum. *J. Comp. Neurol.*, 183, 551−602.

Gwyn, D.G., Nicholson, G.P. and Flumerfelt, B.A. 1977. The inferior olivary nucleus of the rat: a light and electron microscopic study. *J. Comp.*

Neurol., 174,489−520.

Harvey, R.J. and Napper, R.M. 1988. Quantitative study of granule and Purkinje cells in the cerebellar cortex of the rat. *J. Comp. Neurol.,* 274, 151−157.

Kappers, A.C.U., Huber, C.G., Crosby, E.C., 1960. The Comparative Anatomy of the Nervous System of Vertebrates, Including Man. Hafner Publishing Company, New York, vol. 1, pp, 668−695.

Kawamura, K. and Hashikawa, T. 1970. Olivocerebellar projections in the cat studied by means of anterograde axonal transport of labeled amino acids as tracers. *Neuroscience,* 4, 1615−1633.

Kooy, F. H. 1916. The inferior olive in vertebrates. *Fol. Neurobiol.* Leipzig, 10, 205−369.

Kuhlenbeck, H. 1975. pp, 288−623. *In:* The Central Nervous System of the Vertebrates, vol 4, S. Karger, Basal.

Leonard, C.S., Simpson, J.I. and Graf, W. 1988. Spatial organization of visual messages of the rabbit's cerebellar flocculus. I. Topography of inferior olive neurons of the dorsal cap of kooy. *J. Neurophysiol.*, 60,

2073−2090.

Lopez−Roman, A. and Armengol, J.A. 1996. Naturally occurring neuronal death during the development of the inferior olive in the chick. *Neurosci. Res.*, 26, 171−179.

Martin G.F, Dom R, King J.S, Robards M and Watson C.R.R (1975). The inferior olivary nucleus of the opossum (*Didelphis masupialis virginiana*), its organization and connections. *J. Comp. Neurol.,* 160, 507−534.

Mayhew, T.M., MacLaren, R. and Henery, C.C. 1990. Fractionator studies on Purkinje cells in the human cerebellum: numbers in right and left halves of male and female brains. *J. Anat.,* 169, 63−70.

Mlonyeni, M. 1973. The number of Purkinje cells and the inferior olivary neurons in the cat. *J. Comp. Neurol.,* 147, 1−9.

Moatamed, F., 1968. Cell frequencies in the human inferior olivary nuclear complex. *J. Comp. Neurol.,* 128, 109−116.

Mwamengele, G.L., Mayhew, T.M. and Dantzer, V. 1993. Purkinje cell complements in mammalian cerebella and the biases incurred by counting nucleoli. *J. Anat.*, 183, 155−160.

Nairn, J.G., Bedi, K.S., Mayhew, T.M. and Campbell, L.F. 1989. On the number of Purkinje cells in the human cerebellum: unbiased estimates obtained by using the "fractionator". *J. Comp. Neurol.*, 290, 527−532.

Rashed, R., Imagawa, T. and Uehara, M. 2005. A quantitative study of the Purkinje cells in the cerebellum and the inferior olivary neurons in the chicken. *J. Vet. Med. Sci.*, 67, 1261−1263.

Ruigrok, T. J. H., 1997. Cerebellar nuclei: the olivary. The olivary connection. Prog. Brain Res. 114, 167-192.

Ruigrok, T. J. H., 2003. Collateralization of climbing and mossy fibers projection to the nodulus and flocculus of the rat cerebellum. *J. Comp. Neurol.* 466, 278 - 298.

Ruigrok, T.J.H. and Voogd, J. 2000. Organization of projections from the inferior olive to the cerebellar nuclei in the rat. *J. Comp. Neurol.*, 426, 209−228.

Rutherford, J.G. and Gwyn, G. 1980. A light and electron microscopic study of the inferior olivary nucleus of the squirrel monkey, *Saimiri sciureus. J. Comp. Neurol.*, 189, 127−155.

Saigal, R.P., Karamanlidis, A.N., Voogd, J., Michaloudi, H. and Mangana, O. 1983. Olivocerebellar connections in sheep studied with retrograde transport of horseradish peroxidase. *J. Comp. Neurol.,* 217, 440−448.

Schild, R.F. 1970. On the inferior olive of the albino rat. *J. Comp. Neurol.,* 140, 255−260.

Sugihara, I., Shinoda, Y., 2004. Molecular, topographic, and functional organization of the cerebellr cortex: a study with combined aldolase C and olivocerebellar labeling. *J. Neurosci.*, 24, 8771-8785.

Sugihara, I., Wu H.S. and Shinoda, Y. 1999. Morphology of single olivocerebellar axons labeled with biotinylated dextran amine in the rat. *J. Comp. Neurol.*, 414, 129−148.

Sugihara, I., Wu, H.S. and Shinoda, Y. 2001. The entire trajectories of single olivocerebellar axons in the cerebellar cortex and their contribution to cerebellar compartmentalization. *J. Neurosci.,* 21, 7715-7723.

Szentagothai, J. and Rajkovits, U. 1959. Über den ursprung der kletternfasern des kleinhirns. *Z. Anat. Entwickl.*, 121, 120−140.

Taber, E. 1961. The cytoarchitecture of the brain stem of the cat. I. Brain stem nuclei of cat. *J. Comp. Neurol.,* 116, 27−69.

Tan, J., Gerrits, N.M., Nanhoe, R., Simpson, J.I. and Voogd, J. 1995. Zonal organization of the climbing fiber projection to the flocculus and nodulus of the rabbit: a combined axonal tracing and acetylcholinesterase histochemical study. *J. Comp. Neurol., 356*, 23 - 50.

Voogd, J. 2003. The human cerebellum. *J. Chem. Neuroanat.*, 26, 243 - 52.

Voogd, J. and Glickstein, M. 1998. The anatomy of the cerebellum. *Trends Neurosci.,* 21, 370−375.

Voogd, J. and Ruigrok, T.J. 2004. The organization of the corticonuclear and olivocerebellar climbing fiber projections to the rat cerebellar vermis: the congruence of projection zones and the zebrin pattern. *J. Neurocytol.,* 33, 5−21.

Voogd, J., Gerrits, N.M. and Ruigrok, T.J.H. 1996. Organization of the vestibulo-cerebellum. *Ann. N. Y. Acad. Sci.*, 781, 553 - 579.

Voogd, J., Wylie, D.R.W., 2004. Functional and anatomical organization of floccular zones: A preserved feature in vertebrates. *J. Comp. Neurol.,*

470, 107-112.

Voogd - Nilson, L. 1954. The inferior olive in birds. A comparative morphological study. *J. Comp. Neurol.,* 101, 447−481.

Watson, C.R.R. and Herron, P. 1977. The inferior olivary complex of marsupials. *J. Comp. Neurol.,* 176, 527 - 538.

Whitlock, D.G. 1952. A neurohistological and neurophysiological study of afferent fiber tracts and receptive areas of the avian cerebellum. *J. Comp. Neurol.,* 97, 567 - 635.

Whitworh, R.H. and Haines, D.E. 1986. On the question of nomenclature of homologous subdivision of the inferior olivary complex. *Arc. Ital Biol.,* 124, 271 - 317.